A TSUNAMI FORECAST MODEL FOR PALM BEACH, FLORIDA

Edison Gica

February 16, 2014

Table of Contents

List of Tables

List of Figures

FOREWORD

Several Pacific Ocean Basin tsunamis have been recognized as a potential hazard to United States coastal communities since the mid-twentieth century, when multiple destructive tsunamis caused damage to the states of Hawaii, Alaska, California, Oregon, and Washington. In response to these events, the United States, under the auspices of the National Oceanic and Atmospheric Administration (NOAA), established the Pacific and Alaska Tsunami Warning Centers, dedicated to protecting United States interests from the threat posed by tsunamis. NOAA also created a tsunami research program at the Pacific Marine Environmental Laboratory (PMEL) to develop improved warning products.

The scale of destruction and unprecedented loss of life following the December 2004 Sumatra tsunami served as the catalyst to refocus efforts in the United States on reducing tsunami vulnerability of coastal communities, and on 20 December 2006, the United States Congress passed the "Tsunami Warning and Education Act" under which education and warning activities were thereafter specified and mandated. A "tsunami forecasting capability based on models and measurements, including tsunami inundation models and maps" is a central component for the protection of United States coastlines from the threat posed by tsunamis. The forecasting capability for each community described in the PMEL Tsunami Forecast Series is the result of collaboration between the National Oceanic and Atmospheric Administration office of Oceanic and Atmospheric Research, National Weather Service, National Ocean Service, National Environmental Satellite, Data, and Information Service, the University of Washington's Joint Institute for the Study of the Atmosphere and Ocean, National Science Foundation, and United States Geological Survey.

NOAA Center for Tsunami Research

A Tsunami Forecast Model for Palm Beach, Florida

Edison Gica

Abstract

The National Oceanic and Atmospheric Administration has developed a tsunami forecast model for Palm Beach, Florida, as part of an effort to provide tsunami forecasts for United States coastal communities. Development, validation, and stability testing of the tsunami forecast model has been conducted to ensure model robustness and stability. The Palm Beach tsunami forecast model employs the optimized version of the Method of Splitting Tsunami numerical code, and the stability and reliability of the model was tested by simulating artificial tsunamis from different source regions. Six synthetic M_w = 9.4 mega-tsunami events, one M_w = 7.5 synthetic event, and one M_w = 6.2 micro-tsunami event were used, and the forecast model was stable for 24 hours. The Palm Beach forecast model can generate 4 hr of tsunami wave characteristics in approximately 9.7 min of CPU time.

1.0 Background and Objectives

The National Oceanic and Atmospheric Administration (NOAA) Center for Tsunami Research (NCTR) at the NOAA Pacific Marine Environmental Laboratory (PMEL) has developed a tsunami forecasting capability for operational use by NOAA's two Tsunami Warning Centers located in Hawai'i and Alaska (Titov *et al.*, 2005). The system is designed to efficiently provide basin-wide warning of approaching tsunami waves accurately and quickly. The system, termed Short-term Inundation Forecast of Tsunamis (SIFT), combines real-time tsunami event data with numerical models to produce estimates of tsunami wave arrival times and amplitudes at a coastal community of interest. The SIFT system integrates several key components: deep-ocean observations of tsunamis in real time, a basin-wide pre-computed propagation database of water level and flow velocities based on potential seismic unit sources, an inversion algorithm to refine the tsunami source based on deep-ocean observations during an event, and high-resolution tsunami forecast models, hereafter termed forecast models.

This report details the development of a tsunami forecast model for Palm Beach, Florida. Development includes construction of a digital elevation model (DEM) based on available bathymetric and topographic data, model validation with historic events, and stability tests of the model with a suite of mega-tsunami events originating from subduction zones in the Atlantic Ocean.

Palm Beach is a 25.75-km-long barrier island, located on the east side of Palm Beach County, with its eastern side facing the Atlantic Ocean. Three bridges over the Intracoastal Waterway (Flagler Memorial Bridge, Royal Park Bridge, and East State Road 80) connect the island to West Palm Beach (Figure 1). Palm Beach got its name in 1878 from a shipwrecked vessel loaded with coconuts that were bound from Havana to Barcelona. In an effort to launch the region into the commercial coconut industry, early settlers salvaged and planted the coconuts, which were not native to South Florida (Government of Palm Beach, 2011).

In the early nineteenth century, the first settlers started to occupy Palm Beach County. The town of Palm Beach was first incorporated into St. Johns County in 1821. Until its official establishment in 1909, it was part of several counties. It was the second municipality incorporated into Florida's 47th county, Palm Beach County, in 1911. Since 1909, parts of Palm Beach County have been divided among other counties. Palm Beach County is currently defined by water into six physical zones: Atlantic Ocean, barrier islands, lakes and lagoons, sandy flatlands, swamps or marshes, and Lake Okeechobee. Palm Beach County has a very diverse community from different parts of the U.S. and the world. When the U.S. was preparing for possible involvement in World War II, Palm Beach County was viewed as an ideal place to train pilots and test airplanes due to its temperate climate and flat terrain (Palm Beach County, 2011).

The population of Palm Beach County in pre-war 1940 was 80,000; it grew to nearly 115,000 by 1950 and quickly increased from that point on, with a current (2010) population of 1,320,134 (U.S. Census Bureau, 2010). The primary driver of Palm Beach County's economy is tourism, with 3.62 million visitors staying in hotels in 2009. Additionally, the county's production of sweet corn, rice, bell peppers, lettuce, radishes, Chinese vegetables, specialty leaf, celery, and sugar cane is ranked first in Florida due to its year-round sunny climate. The presence of companies like B/E Aerospace, Lockheed Martin, and Sikorsky Aircraft are indicative of Palm Beach County's prominence in the aerospace, aviation, and engineering industries. The life sciences are also well represented, with regional offices of organizations such as Scripps Research Institute and Max Planck Society. The region will soon become the second largest supplier of "utility-scale" solar power in the nation, when NextEra's Next Generation Solar Energy Center is completed. Palm Beach County was ranked third in Forbes' list of "Hotbeds of Tomorrow's Technology." With affluent towns and leading industries in its region, it is the wealthiest county in Florida, with an average per capita personal income of $58,358 (Delta Skyway Magazine, 2010). The town of Palm Beach has a population of just 8348 (U.S. Census Bureau, 2010), but with its median family income of $137,867 and per capita income of $109,219 (U.S. Census Bureau, 2010), it is the wealthiest community in the State of Florida, and one of the most affluent in the entire U.S. (Delta Skyway Magazine, 2010).

2.0 Forecast Methodology

A high-resolution inundation model was used as the basis for operational development of a tsunami forecast model to provide an estimate of wave arrival time, wave height, and inundation at Palm Beach, Florida, following tsunami generation. All tsunami forecast models are run in real time while a tsunami is propagating across the open ocean. The Palm Beach model was designed and tested to perform under stringent time constraints, given that time is generally the single limiting factor in saving lives and property. The goal of this work is to maximize the length of time that the community of Palm Beach has to react to a tsunami threat by providing accurate information quickly to emergency managers and other officials responsible for the community and infrastructure.

The general tsunami forecast model, based on the Method of Splitting Tsunami (MOST), is used in the tsunami inundation and forecasting system to provide real-time tsunami forecasts at selected coastal communities. The model runs in minutes while employing high-resolution grids

constructed by the National Geophysical Data Center (NGDC). MOST is a suite of numerical simulation codes capable of simulating three processes of tsunami evolution: earthquake, transoceanic propagation, and inundation of dry land. The MOST model has been extensively tested against a number of laboratory experiments and benchmarks (Synolakis *et al.*, 2008) and was successfully used for simulations of many historical tsunami events. Titov and González (1997) describe the technical aspects of forecast model development, stability, testing, and robustness, and Tang *et al*., 2009 provide detailed forecast methodology.

A basin-wide database of pre-computed water elevations and flow velocities for unit sources covering worldwide subduction zones has been generated to expedite forecasts (Gica *et al.*, 2008). As the tsunami wave propagates across the ocean and successively reaches tsunameter observation sites, recorded sea level is ingested into the tsunami forecast application in near real time and incorporated into an inversion algorithm (Percival *et al.*, 2011) to produce an improved estimate of the tsunami source. A linear combination of the pre-computed database is then performed based on this tsunami source, now reflecting the transfer of energy to the fluid body, to produce synthetic boundary conditions of water elevation and flow velocities to initiate the forecast model computation.

Accurate forecasting of the tsunami impact on a coastal community largely relies on the accuracies of bathymetry and topography and the numerical computation. The high spatial and temporal grid resolution necessary for modeling accuracy poses a challenge in the run-time requirement for real-time forecasts. Each forecast model consists of three nested grids with increasing spatial resolution in the finest grid, and temporal resolution for simulation of wave inundation onto dry land. The forecast model utilizes the most recent bathymetry and topography available to reproduce the correct wave dynamics during the inundation computation. Forecast models, including the Palm Beach model, are constructed for at-risk populous coastal communities in the Pacific and Atlantic oceans. Previous and present development of forecast models in the Pacific (Titov *et al*., 2005; Titov, 2009; Tang *et al*., 2009; Wei *et al*., 2008) have validated the accuracy and efficiency of each forecast model currently implemented in the real-time tsunami forecast system. Models are tested when the opportunity arises and are used for scientific research.

3. Model Development

The general methodology for modeling at-risk coastal communities is to develop a set of three nested grids, referred to as A, B, and C grids, each of which becomes successively finer in resolution as they telescope into the population and economic center of the community of interest. The offshore area is covered by the largest and lowest-resolution A grid, while the near-shore details are resolved within the finest-scale C grid, to the point that tide gauge observations recorded during historical tsunamis are resolved within expected accuracy limits. The procedure is to begin development with large spatial extent merged bathymetric/topographic grids at high resolution, and then optimize these grids by subsampling to coarsen the resolution and reduce the overall grid dimensions to achieve a 4 hr simulation of modeled tsunami waves within the required time period of 10 min of wall-clock time. The basis for these grids is a high-resolution digital elevation model (DEM), constructed by the NGDC and NCTR using all available

bathymetric, topographic, and shoreline data, to reproduce the wave dynamics during the inundation computation for an at-risk community. For each community, data are compiled from a variety of sources to produce a DEM referenced to Mean High Water in the vertical and the World Geodetic System (WGS) 1984 in the horizontal (http://ngdc.noaa.gov/mgg/inundation/tsunami/inundation.html). As new DEMs become available, forecast models will be updated and report updates will be posted at http://nctr.pmel.noaa.gov/forecast_reports/. From these DEMs, a set of three high-resolution, "reference" elevation grids are constructed, as shown in Figure 2, for development of a high-resolution reference model, from which an "optimized" model is constructed to run in an operationally specified period of time. This model is referred to as the optimized tsunami forecast model, or forecast model for brevity.

A significant portion of the modeled tsunami waves, 24 hr of modeled tsunami time, for Palm Beach, Florida, pass through the model domain without appreciable signal degradation. Table 1 provides specific details of both high-resolution reference and tsunami forecast model grids, including extents, and Appendix A provides complete input parameter information for the model runs.

3.1 Forecast area

The Intracoastal Waterway is connected to the Atlantic Ocean through several inlets. The widest inlet is located between the town of Palm Beach and Palm Beach Shores (Figure 1). Several islands are located inside the Intracoastal Waterway: Munyon Island, Little Munyon Island, Singer Island, Peanut Island, Everglades Island, Tarpon Island, Fisherman Island, Bingham Island, Hunters Island, Ibis Isle, and Hypoluxo Island. There are also water inlets that go further inland. The coast is lined with piers and docks. The former site of the Port of West Palm Beach tide gauge (identified in Figure 3) marks the location of greatest water depth (13 m) within the inlet. The shallowest depths (1 m) are generally found inside boat docking areas. Water depth at the entrance of the inlet between Palm Beach Shores and Palm Beach is approximately 17 m.

The proximity of the 25.75 km barrier island town of Palm Springs to the Gulf Stream contributes to its outstanding marine environment, lush gardens, and palm-lined beaches (Government of Palm Beach, 2011). The highest elevation of the town of Palm Beach is close to 6 m, where most of the highest elevation points are fronting the Atlantic Ocean. The town's lowest elevation is just under 1 m. As can be seen in Figure 3, the majority of the island barrier is just a few meters above water. A land elevation of just under 1 m can easily be inundated by a large tsunami, and tsunami waves can quickly fill the Intracoastal Waterway and inundate the eastern side of Palm Beach County. For this reason, the forecast area also includes municipalities west of the Intracoastal Waterway, including the communities of Cloud Lake, Glen Ridge, Greenacres, Haverhill, Hypoluxo, Lake Clarke Shores, Lake Park, Lake Worth, Lantana, Manalapan, Mangonia Park, North Palm Beach, Palm Beach Gardens, Palm Beach Shores, Palm Springs, Riviera Beach, South Palm Beach, and West Palm Beach (Figure 4). The total population of the forecast area is 315,666 (U.S. Census Bureau, 2010). The highest elevation of all the included municipalities is close to 13 m, but these are isolated to a small area; the general elevation is mostly below 6 m (Figure 3).

3.2 Historical events and data

The U.S. East Coast is most susceptible to earthquakes and tsunamis generated from the Azores-Gibraltar plate boundary, located in the northern basin of the Atlantic Ocean. The 1 November 1775 Lisbon earthquake was the largest tsunamigenic earthquake that occurred, with an estimated magnitude (Mw) of 8.5–9.0 (ten Brink *et al.*, 2008). Fortunately, no tsunamigenic earthquake has occurred since then. This absence of events makes it more difficult to validate the forecast model for Palm Beach, but the historical tsunami source can still be used to simulate the generated tsunami waves and determine how Palm Beach is affected.

Even if there were historical accounts of the 1775 Lisbon tsunami, no tide gauge was established in Palm Beach to record that data. The Port of West Palm Beach had a tide gauge installed in the Intracoastal Waterway at 80° 3.1’ W, 26° 46.2’ N (Figure 3) on 1 May 1967. It was removed on 17 April 1969, reinstalled on 24 January 2008, and removed again on 20 October 2010. Currently, the closest tide gauge station is in Lake Worth Pier at 80° 2’ W, 26° 36.7’ N, which is in the open ocean facing the Atlantic Basin (Figure 3). The closest point selected in the forecast model DEM as the tide gauge location is at 80° 1’ 59.86” W, 26° 36’ 42.33” N, with a depth of 4.74 m. This site was established on 14 April 1970, but the present installation was completed on 1 June 2010. The tide gauge at Lake Worth Pier has a mean range of 0.832 m and a diurnal range of 0.918 m. The station also shows that there is a mean sea level difference of 0.06 m from a record range of 1960–1978 to 1983–2001 (Tides and Currents, 2011).

3.3 Model setup

One unique feature of the U.S. East Coast is the existence of a very wide continental shelf. Additionally, there are several islands (The Bahamas) located offshore of the town of Palm Beach (Figure 5). Without careful selection of the domain size of the A grid, the existence of the continental shelf and several islands could potentially affect the simulated tsunami waves in the finest-scale, nearshore grid C. A total of three domain sizes were tested to determine if the extent of the A grid would generate significant variation in the simulated tsunami waves. The DEM used for testing the domain extent of the A grid, with its 9-arc-sec grid resolution covering the U.S. East Coast, the Gulf Coast, and the Caribbean, was developed by NGDC (NGDC, 2005). The smallest A grid is within the continental shelf, with the deepest depth of 825.5 m. The largest A grid extends beyond the continental shelf and well beyond into the deep ocean, with a depth of 5400 m. The medium-size grid is just outside the continental shelf, with a maximum depth of 5000 m (Table 2 and Figure 6). A synthetic Mw 9.5 scenario was used to generate the tsunami waves propagating into the A grid with the epicenter indicated in Figure 7.

The results of testing three different domain sizes for A grid show a slight variation in the simulated tsunami wave height. Time series plots and the maximum tsunami wave amplitude distribution are compared at seven locations, shown in Figure 8; Figure 9a compares the time series and Figure 9b compares the maximum tsunami wave amplitude. The three different grid A sizes indicate a very minimal variation in the tsunami waves, and since the main objective of developing a forecast model is to provide a quick estimate of tsunami wave characteristics (i.e., wave arrival time, wave height, and inundation) minutes following a tsunami event, the smallest grid A (with less computational nodes) will be used in the forecast model.

The high-resolution DEM for Palm Beach was developed by NGDC (Friday *et al.*, 2010) with a grid resolution of 1/3 arc sec and coverage from 80.3600°W to 79.4200°W and 26.2900°N to 27.3100°N (Figure 2). The deepest water depth covered by the domain is 796.3 m and the highest topography elevation is 26.37 m. The DEM for the high-resolution reference and forecast models were extracted directly from the DEM developed by NGDC.

The coverage extent of both high-resolution reference and forecast models are the same. Table 1 shows the details of the nested grids (A, B, and C), including the modeling parameters used. The plots of the nested grids are shown in Figure 10. The outermost grid (A) covers the deep ocean region to capture the tsunami characteristics as it propagates in the deep ocean, while the innermost grid (C) captures the tsunami wave transformation in the shallow water area The forecast model, which is used for tsunami forecasting during an event, is designed so that it can quickly provide 4 hr of simulated tsunami wave characteristics, including time series at the tide gauge. For the town of Palm Beach, the forecast model can simulate the 4 hr of tsunami wave characteristics in approximately 9.7 min (Table 1). The high-resolution reference model, on the other hand, takes about 3.3 hr to complete a simulated run of 4 hr. Neither the high-resolution reference model nor the forecast model was validated with historical events to check for accuracy since no historical records/accounts exist. However, simulations of historical sources were done to determine how a tsunami would affect the town of Palm Beach. The stability and reliability of both high-resolution reference and forecast models were tested by running synthetic scenarios of different earthquake magnitudes (Mw 9.4, 7.5, and 6.2) as listed in Table 3, with Figure 11 showing their locations.

4. Results and Discussion

4.1 Model validation

The development of the DEM for the high-resolution reference model and forecast model requires that it be validated to determine the accuracy of the simulated tsunami characteristics as it reaches the coastal areas of Palm Beach, Florida. As discussed in Section 3.2, the historical tsunami source for the 1775 Lisbon event is considered for validation purposes. Although no historical tide gauge data or accounts are available, the historical tsunami source (ten Brink *et al*., 2008) can be used to determine how the generated tsunami wave would affect Palm Beach.

The other method to validate the forecast model is to compare the tsunami wave characteristics with the high-resolution reference model. A higher-resolution DEM should provide finer distributions of the tsunami wave pattern that might not be reflected in a forecast model due to a coarser resolution. Since the forecast model is designed to provide a quick forecast, this coarser resolution is needed but the deviation with the higher-resolution reference model should not be too significant. Comparison between the forecast model and high-resolution reference model will be evaluated by looking at the tide gauge time series and distribution of the maximum tsunami wave amplitude in grids A, B, and C.

4.2 Model stability and reliability

The forecast model must provide a reliable forecast and should be stable enough to simulate several hours of the tsunami event. Reliability and stability tests were conducted by simulating synthetic events emanating from different regions and using different earthquake magnitudes (Mw= 9.4, 7.5, and 6.2). Since each tsunami event is unique, tests using different earthquake magnitudes and source locations would indicate if the developed model will generate instabilities that need to be corrected. This set of tests is not exhaustive, but representative cases from select sources should be sufficient. A total of five artificial mega-tsunamis (Mw=9.4) were generated using 20 unit sources with a slip value of 30 m for each unit source. One case of Mw=7.5 used one unit source with a slip of 1 m, and for a small wave condition, one case of Mw=6.2 with a slip of 0.01 m was simulated. The unit sources are from the propagation database developed at NCTR (Gica *et al.*, 2008). Tests were conducted for a total of 24 hr simulation. The sources used in these tests are listed in Table 3 for the synthetic Mw 9.4, Mw 7.5, and Mw 6.2 events. The locations of these sources in relation to Palm Beach are shown in Figure 11.

4.3 Results of tested events

For validation purposes, the reference and forecast models must be compared with historical events. However, there are no historical records for Palm Beach; not even for the 1755 Lisbon tsunami, which was documented in Europe. Validation must therefore be done by comparing the simulated tsunami wave characteristics between the high-resolution reference and forecast models, since it is expected that the higher resolution would provide a finer distribution of tsunami wave patterns. The tsunami time series for reference and forecast models compare very well at Lake Worth Pier tide gauge (Figure 12). The mega-tsunami event scenarios emanating from the Caribbean region generated an almost perfect match for the entire time series at the selected warning point (Figures 13-18). The mega-tsunami event scenarios from ATSZ 38-48 (Figure 13) and South Sandwich Island (SSSZ 1-10, Figure 18) displayed slight variation in the later waves. For all mega-tsunami events and the 1755 Lisbon runs, the maximum tsunami wave amplitude distribution between the reference and forecast models at the A-, B-, and C-grid levels are very similar. (Figures 13–18 show representative results for the C-grid level.) The similarity persists inside the Intracoastal Waterway for all scenarios at the C-grid level, with slight differences found at the inlet entrance between Palm Beach and Palm Beach Shores and Peanut Island (Figure 1). The deeper waters found in this section, which are used by ships to navigate into the Port of West Palm Beach, and the relatively long, narrow entrance into the Intracoastal Waterway require a much higher-resolution grid to better resolve the tsunami wave characteristics. In Figures 13–18, the forecast model (using a coarser grid resolution of 2 arc sec) consistently shows a slightly higher (less than 5 cm) distribution of maximum tsunami wave amplitude as compared with the reference model, which uses 2/3 arc sec.

The simulated synthetic events (Mw=9.4, 7.5, and 6.2) show that the forecast model is stable. Although the mega-tsunami (Mw 9.4) tests are not exhaustive, the results can indicate which tsunami source regions are most likely to pose a threat to Palm Beach. Simulated results indicate that source scenarios (mega-tsunami events) ATSZ 48–57 (Figure 14) and ATSZ 58–67 (Figure 15) generated much higher tsunami waves offshore of Palm Beach as compared to other synthetic mega-events tested. The higher offshore tsunami waves are due to the two mega-

tsunami events (ATSZ 48–57 and ATSZ 58–67) being located on the northern end of the Caribbean region and oriented more toward Palm Beach (Figure 11). However, all the simulated mega-tsunami events show that Palm Beach is safe from seismically generated tsunamis emanating from the Caribbean and Europe (based on model results from the 1755 Lisbon tsunami). The incoming tsunami waves arriving along the coast and entering the Intracoastal Waterway barely generate any inundation. The tsunami energy generated from the synthetic events in the Caribbean is trapped inside the Caribbean Sea with very minimal energy leaking out. Although there are quite a number of sources (Gica *et al.*, 2008) along the northeast and east side of Palm Beach facing the Atlantic Ocean, the large continental shelf and the Bahamas to the east block and quickly dissipate the tsunami energy. The wide continental shelf was also found to play a role in minimizing the impact of tsunami waves on Palm Beach during the 1755 Lisbon tsunami.

5. Summary and Conclusion

Reference and forecast models have been prepared for Palm Beach, Florida. During the development of these models, instabilities occurred due to the existence of extreme shallow regions inside the Intracoastal Waterway. These locations were corrected, either manually or by smoothing a cluster of nodes if the single node causing the instability could not located. Although there were corrections made to the DEM, both reference and forecast models were found to be stable and the comparison between the models showed good comparison at the tide gauge station and in the distribution of the maximum tsunami wave amplitude for all of the grids (i.e., A, B, and C).

The stability tests show that the forecast model is stable for a 24 hr simulation for synthetic sources with different earthquake magnitudes (Mw = 9.4, 7.5, and 6.2) from different source regions. A total of six Mw 9.4, one Mw 7.5, and one Mw 6.2 events were simulated. The mega-tsunami (Mw 9.4) events not only check the stability of the forecast model, but can also provide information on which source regions present the greatest tsunami risk to Palm Beach. The limited test scenarios conducted show that the continental shelf and islands in the Bahamas (east of Palm Beach) act as a buffer, quickly dissipating the tsunami energy, thus minimizing the effects on Palm Beach. A couple of the test scenarios (i.e., ATSZ 58–67 and ATSZ 68–77) did indicate some minor inundation north of Singer Island (Figure 1 for location and Figures 15 and 16 for inundation) for the high-resolution reference model, but this should not be of much concern since, in reality, there is a water passageway north of Singer Island (Figure 19) that the grid resolution did not fully capture. The minor inundation in the simulation, therefore, does not represent real inundation. The simulation of the 1755 Lisbon tsunami indicated that, should the same scenario occur in the present, it would not pose a threat to Palm Beach.

Since the main objective of developing the Palm Beach forecast model is to forecast a tsunami, the DEM has been optimized to simulate 4 hr of tsunami wave characteristics in approximately 9.7 min. As presented in this report, the Palm Beach forecast model should be able to provide a reliable forecast during an event and is stable for a 24 hr simulation.

6.0 Acknowledgments

This work is funded by the Joint Institute for the Study of the Atmosphere and Ocean (JISAO) under NOAA Cooperative Agreement Numbers NA10OAR4320148 and NA08OAR4320899, and is JISAO Contribution No. 2080. This work is also Contribution No. 3399 from NOAA/Pacific Marine Environmental Laboratory. The author would also like to thank Lindsey Wright (for retrieving historical tide gauge data and testing of the forecast model in SIFT as reported in Appendix C) and Sandra Bigley (for comments, edits and formatting of this report).

7.0 References

Delta Skyway magazine, Dec 2010 issue (DeltaSkywayMag.delta.com), accessed 2011.

Friday, D. Z., L. A. Taylor, B. W. Eakins, K. S. Carignan, R. J. Caldwell, P. R. Grothe, and E. D. Lim (2010): Digital Elevation Models of Palm Beach, Florida: Procedures, Data Sources and Analysis. NOAA Technical Memorandum NESDIS NGDC.

Gica, E., M. C. Spillane, V. V. Titov, C. D. Chamberlin, and J. C. Newman (2008): Development of the forecast propagation database for NOAA's Short-term Inundation Forecast for Tsunamis (SIFT), NOAA Tech. Memo OAR PMEL139, NOAA/Pacific Marine Environmental Laboratory, Seattle, WA, 89 pp.

Government of Palm Beach, Florida, http://palmbeach.govoffice.com, accessed 2011.

NGDC (National Geophysical Data Center) (2005): East Coast and Gulf Coast and Caribbean Nine Second Tsunami Propagation Grids Compilation Report, 1 Dec 2005.

Palm Beach County, http://www.pbchistoryonline.org, accessed 2011.

Percival, D.B., D.W. Denbo, M.C. Eble, E. Gica, H.O. Mofjeld, M.C. Spillane, L. Tang, and V.V. Titov (2011): Extracting tsunami source parameters via inversion of DART buoy data, *Nat. Hazards*, 58(1), doi: 10.1007/s11069-010-9688-1, 567–590.

Synolakis, C. E., E. N. Bernard, V. V. Titov, U. Kânoğlu, and F. I. González (2008): Validation and verification of tsunami numerical models. *Pure and Applied Geophysics,* 165(11–12), 2197–2228.

Tang, L., V. V. Titov, and C. D. Chamberlin (2009): Development, testing, and applications of site-specific tsunami inundation models for real-time forecasting. *J. Geophys. Res.*, *114*, C12025, doi: 10.1029/2009JC005476.

Ten Brink, U., D. Twichell, E. Geist, J. Chaytor, J. Locat, H. Lee, B. Buczkowski, R. Barkan, A. Solow, B. Andrews, T. Parsons, P. Lynett, J. Lin, and M. Sansoucy (2008): Evaluation of Tsunami Sources with the Potential to Impact the U.S. Atlantic and Gulf Coasts, An Updated Report to the Nuclear Regulatory Commission, by the Atlantic and Gulf of Mexico Tsunami Hazard Assessment Group, revised 22 August 2008.

Tides and Currents, wwwtidesandcurrents.noaa.gov, accessed 2011.

Titov, V. V. (2009): Tsunami forecasting. In *The Sea*, Vol. 15, Chapter 12, Harvard University Press, Cambridge, MA, and London, England, 371–400.

Titov, V. V. and F. I. Gonzalez (1997): Implementation and testing of Method of Splitting Tsunami (MOST) model. NOAA Tech. Memo. ERL PMEL-112 (PB98-122773), NOAA/Pacific Marine Environmental Laboratory, Seattle, WA, 11 pp.

Titov, V. V., F. I. Gonzalez, E. N. Bernard, M. C. Eble, H. O. Mofjeld, J. C. Newman and A. J. Venturato (2005): Real-time tsunami forecasting: Challenges and solutions. *Natural Hazards*, 35, 41–58.

U.S. Census Bureau (2010): factfinder2.census.gov, accessed 2011.

Wei, Y., E. Bernard, L. Tang, R. Weiss, V. Titov, C. Moore, M. Spillane, M. Hopkins, and U. Kânoğlu (2008): Real-time experimental forecast of the Peruvian tsunami of August 2007 for U.S. coastlines. *Geophys. Res. Lett., 35*, L04609, doi: 10.1029/2007GL032250.

Table 1. MOST setup parameters for reference and forecast models for Palm Beach, Florida.

		Reference Model				Forecast Model			
Grid	Region	Coverage Lat. [ºN] Lon. [ºW]	Cell Size [“]	nx x ny	Time Step [sec]	Coverage Lat. [ºN] Lon. [ºW]	Cell Size [“]	nx x ny	Time Step [sec]
A	Southeast Florida	27.5000-25.8000 279.0000-280.5000	9	601 x 681	2.0	27.5000-25.8000 279.0000-280.5000	18	301 x 341	4.0
B	Palm Beach County	27.0000-26.4000 279.7500-280.1500	6	241 x 361	2.0	27.0000-26.4000 279.7500-280.1500	9	161 x 241	4.0
C	Palm Beach, FL	26.8482-26.5666 279.8332-279.9999	2/3	901 x 1522	0.4	26.8482-26.5666 279.8332-279.9999	2	301 x 508	1.0
Minimum offshore depth [m]				1.0				1.0	
Water depth for dry land [m]				0.1				0.1	
Friction coefficient [n^2]				0.0009				0.0009	
CPU time for 4-hr simulation				3.3 hours				9.7 minutes	

Computations were performed on a Dell PowerEdge R510 with 2xHex-core Intel Xeon E5670 CPU processor at 2.93 GHz with 12M cache each.

Table 2. Grid extents used to determine the final A-grid size in the development of a forecast model and high-resolution reference model for Palm Beach, Florida.

Test A-Grid	Coverage Lat. [ºN] Lon. [ºW]	Cell Size ["]	nx x ny	Maximum Offshore Depth [meters]
Large	27.5000-25.8000 279.0000-287.0000	9	3201 x 681	5,400.0
Medium	27.5000-25.8000 279.0000-284.5000	9	2201 x 681	5,000.0
Small	27.500-25.8000 279.0000-280.5000	9	601 x 681	825.5

Table 3. Synthetic tsunamis tested for Palm Beach, Florida.

Scenario Name	**Subduction Zone**	**Tsunami Source**	**Mw**
ATSZAB 38-47	Atlantic	30 x (A38-47, B38-47)	9.4
ATSZAB 48-57	Atlantic	30 x (A48-57, B48-57)	9.4
ATSZAB 58-67	Atlantic	30 x (A58-67, B58-67)	9.4
ATSZAB 68-77	Atlantic	30 x (A68-77, B68-77)	9.4
ATSZAB 82-91	Atlantic	30 x (A82-91, B82-91)	9.4
SSSZAB 1-10	South Sandwich	30 x (A1-10, B1-10)	9.4
ATSZB52	Atlantic	1 x B52	7.5
SSSZB11	South Sandwich	0.01 x B11	6.2

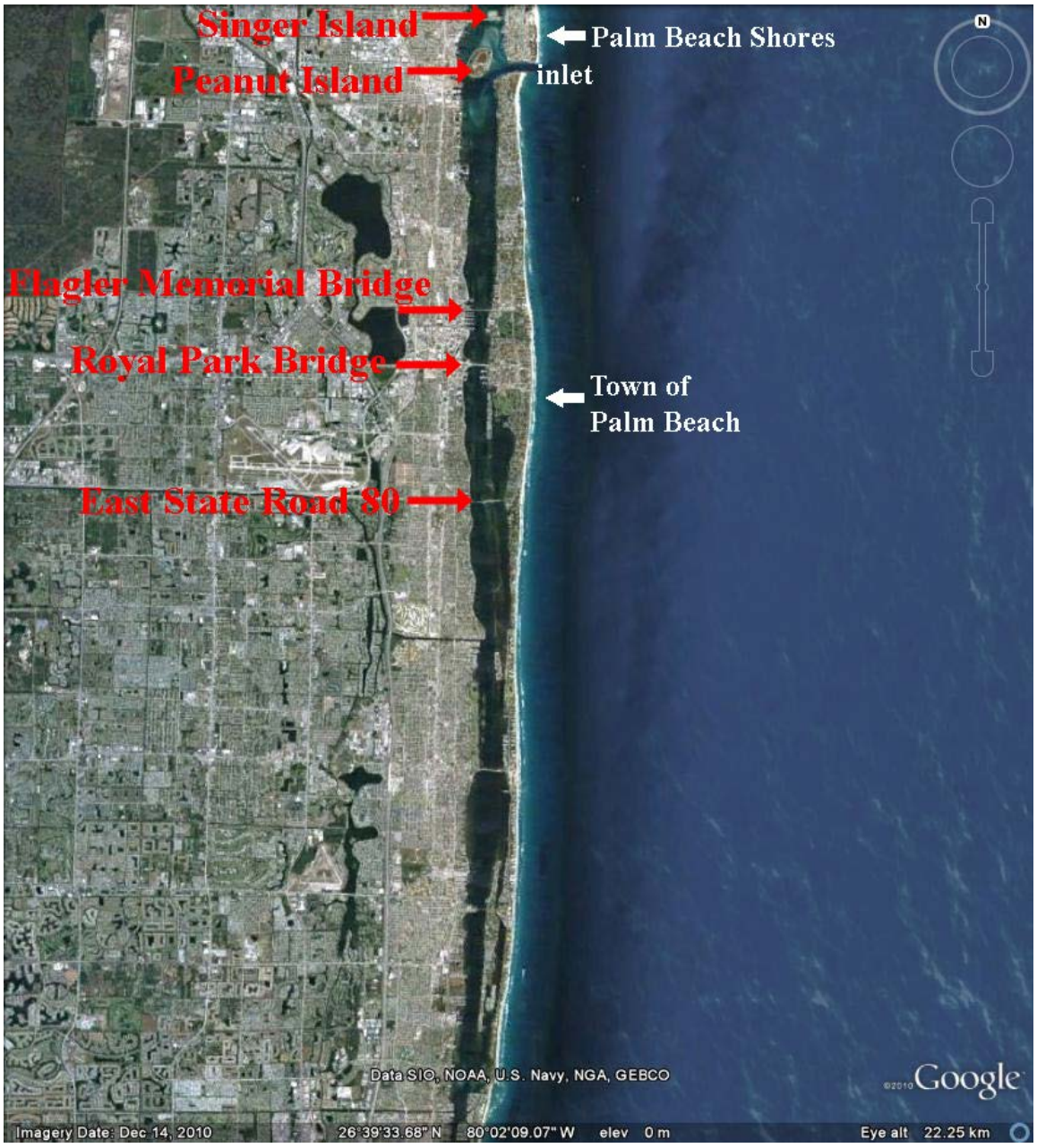

Figure 1. Google map image of Palm Beach, Florida, with the location of the inlet into the Intracoastal Waterway and the three bridges (Flagler Memorial Bridge, Royal Park Bridge, and East State Road 80) that connect the town to West Palm Beach on the western side.

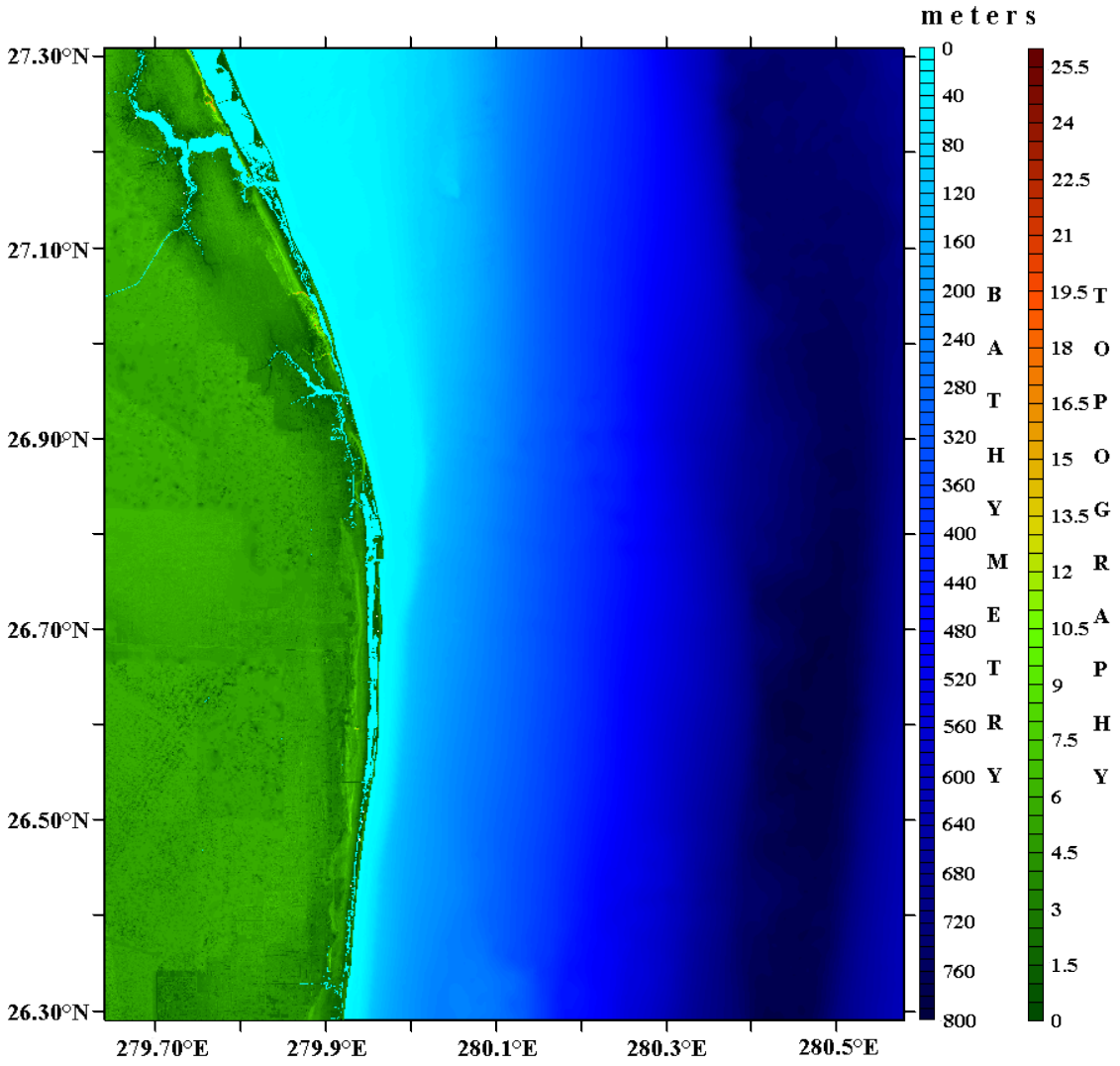

Figure 2. Plot of 1/3 arc sec DEM developed by NGDC and used in the development of the forecast model.

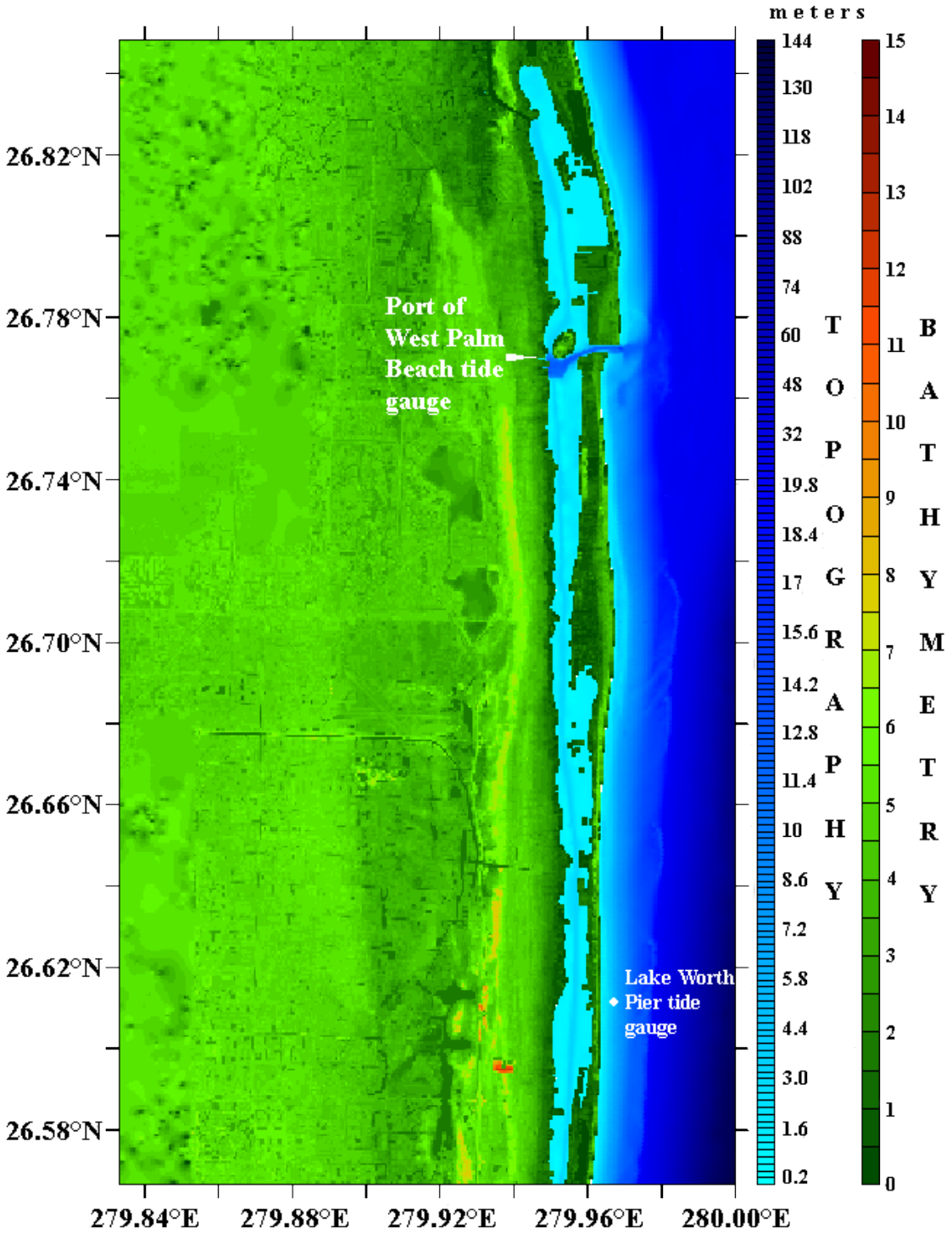

Figure 3. Plot of C-grid extent used in the development of the forecast model based on a 1/3-arc-sec DEM developed by NGDC. The plot also indicates the location of tide gauges in the region (Lake Worth Pier and Port of West Palm Beach). The tide gauge at Port of West Palm Beach was removed on 20 October 2010 (Tides and Currents, 2011).

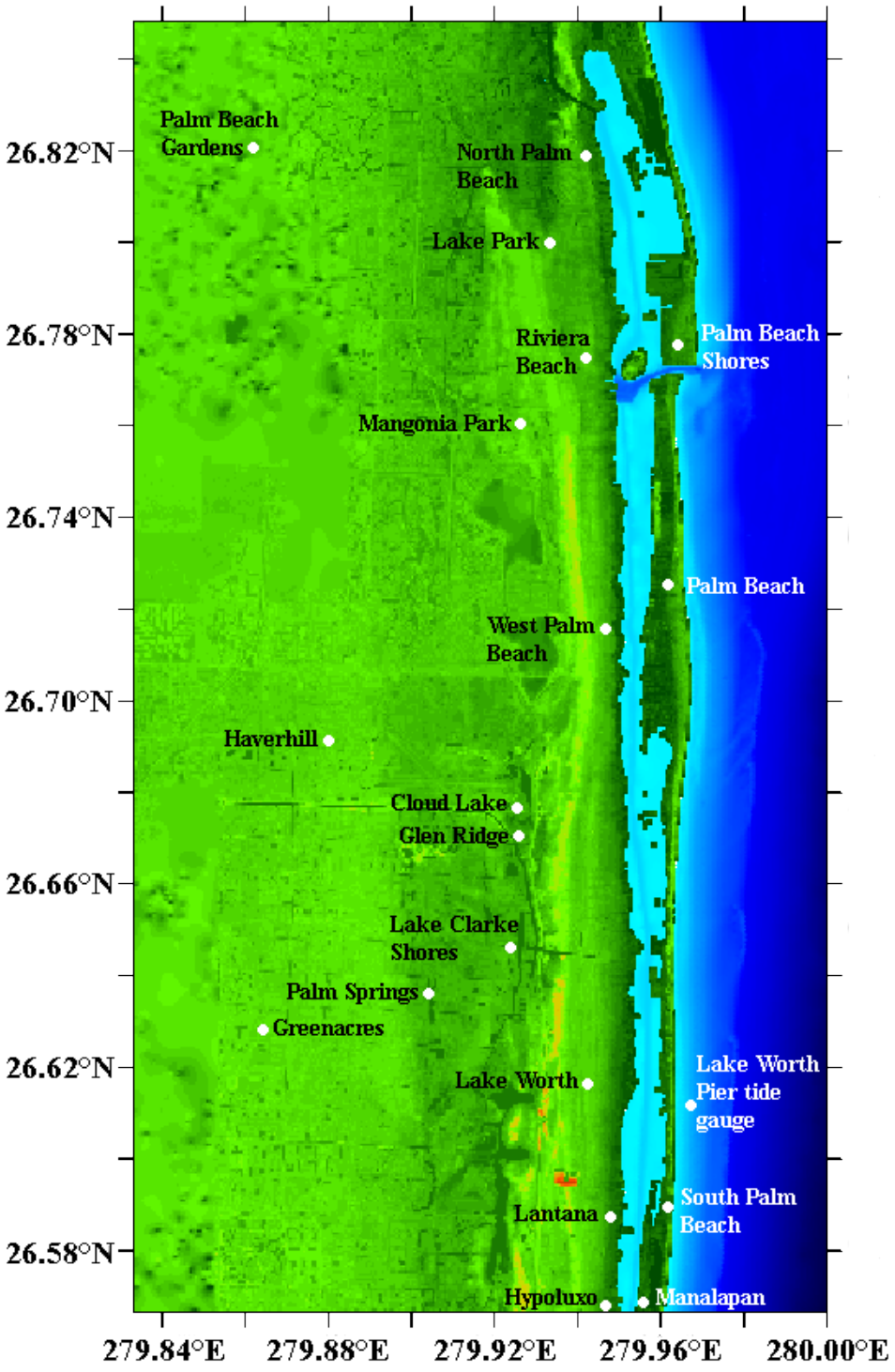

Figure 4. Plot of C-grid extent used in the development of the forecast model indicating cities and towns that are included.

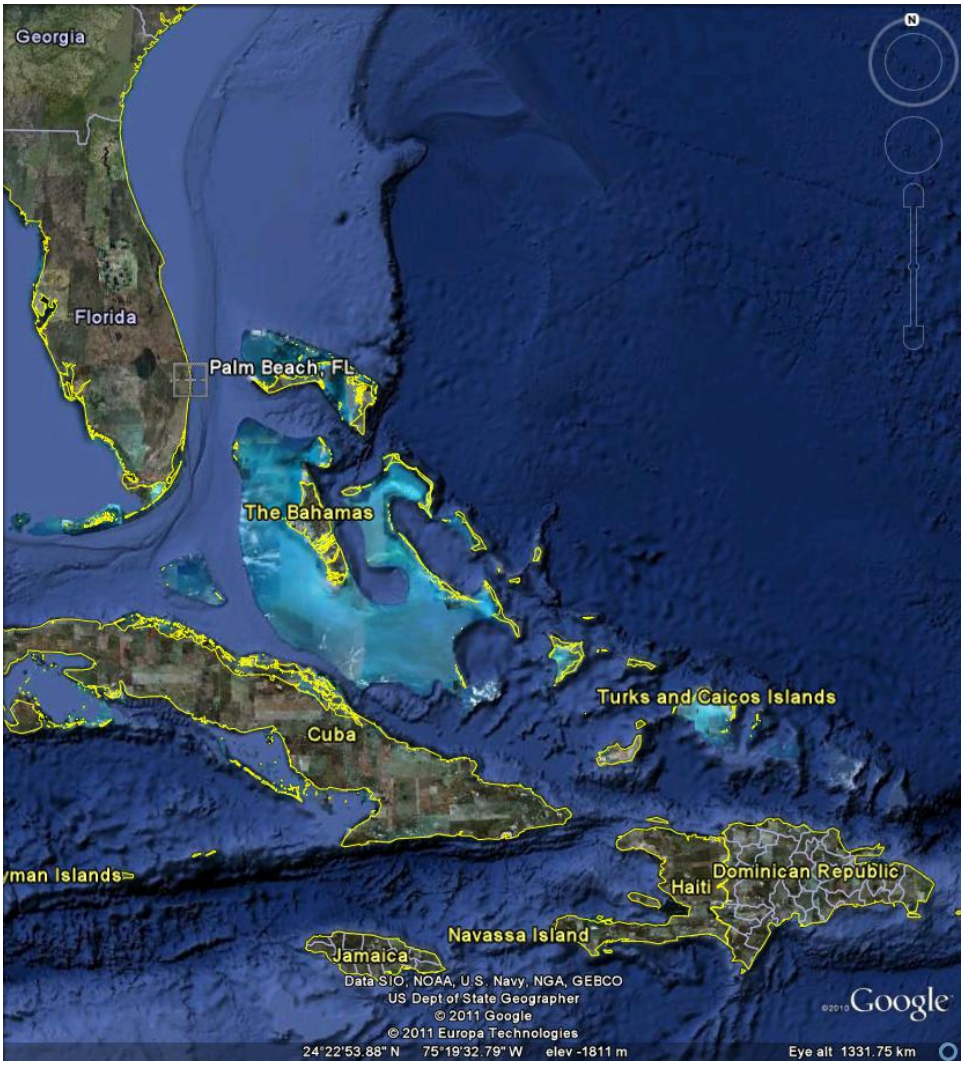

Figure 5. Google map image showing the existence of the wide continental shelf and islands in the Bahamas relative to the location of Palm Beach, Florida.

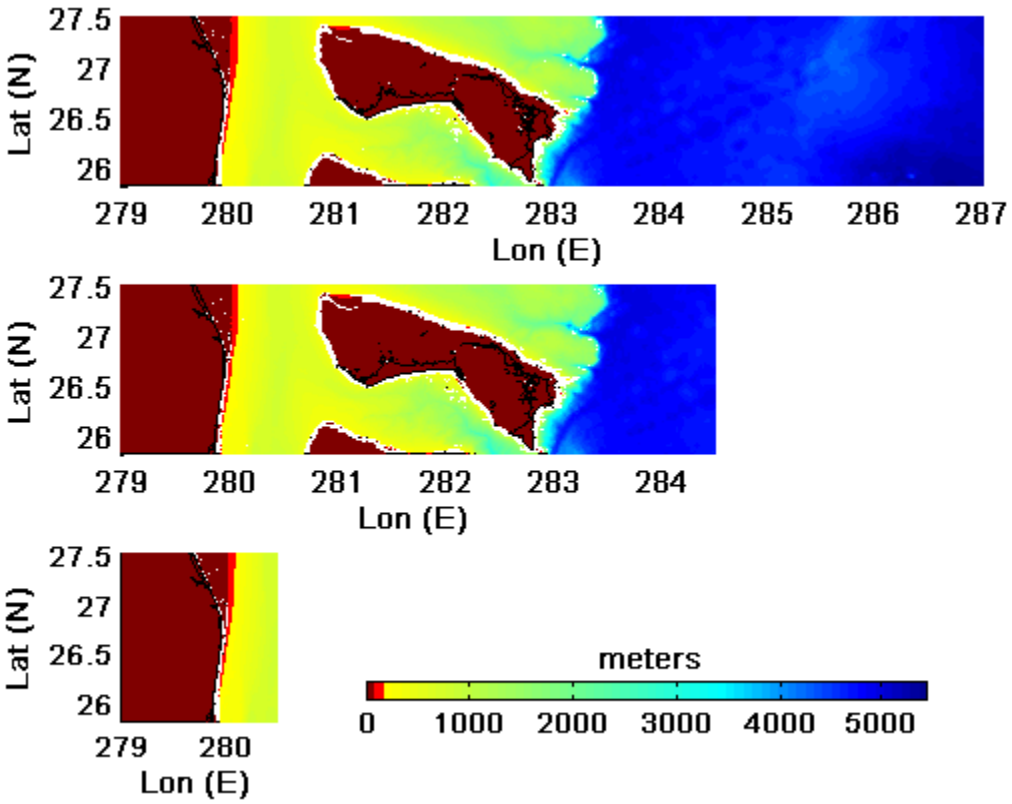

Figure 6. Plots of grid extent used to determine the final A-grid size in the development of a forecast model and high-resolution reference model. The top panel shows the largest grid, covering a significant portion of the deep ocean; the middle panel shows a medium-size grid that still includes deep ocean; the bottom panel is the smallest grid, covering the area along the continental shelf off the coast of Palm Beach.

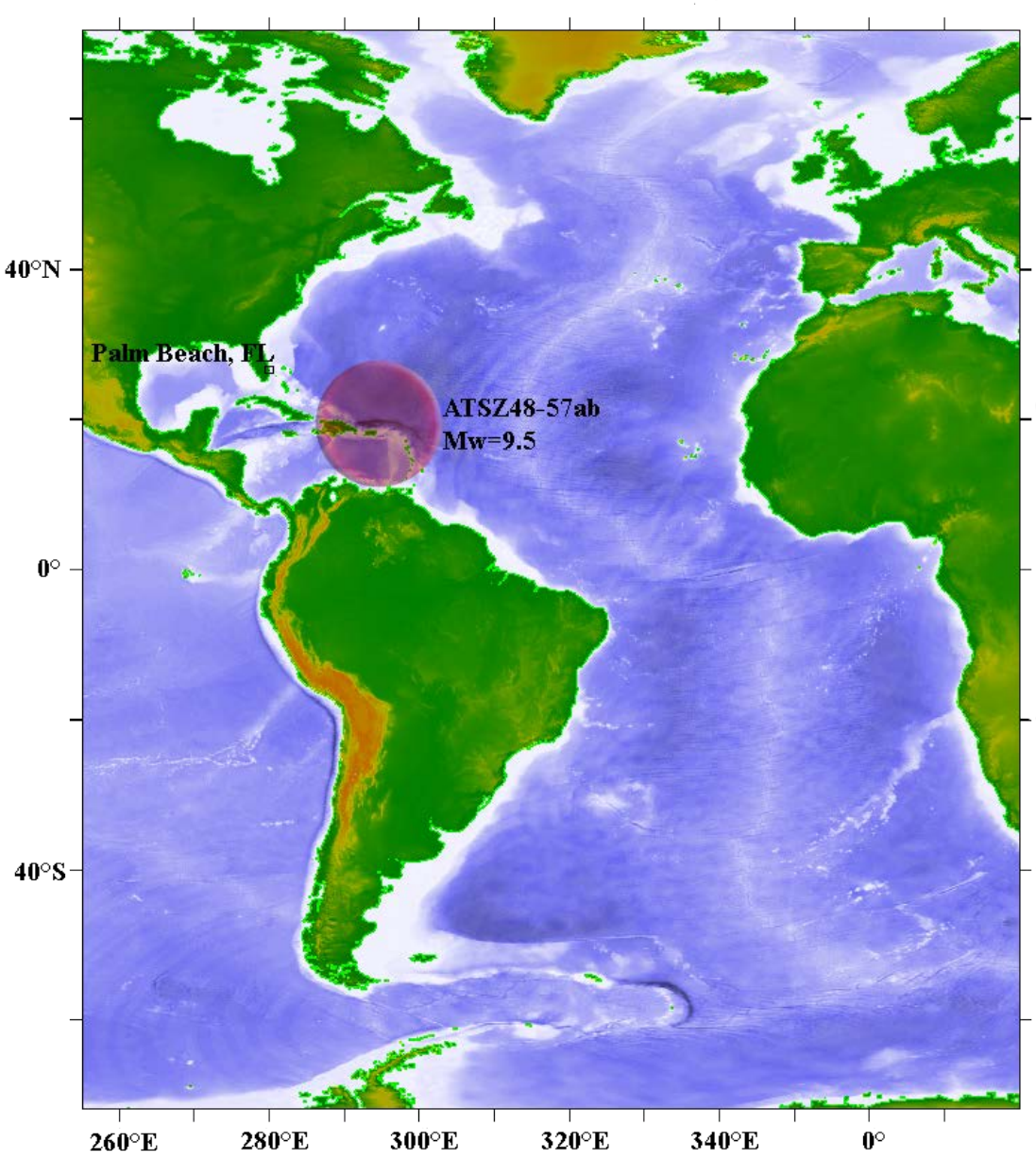

Figure 7. Location of a synthetic mega-tsunami (Mw=9.5) scenario, relative to Palm Beach, Florida, used to test the domain size.

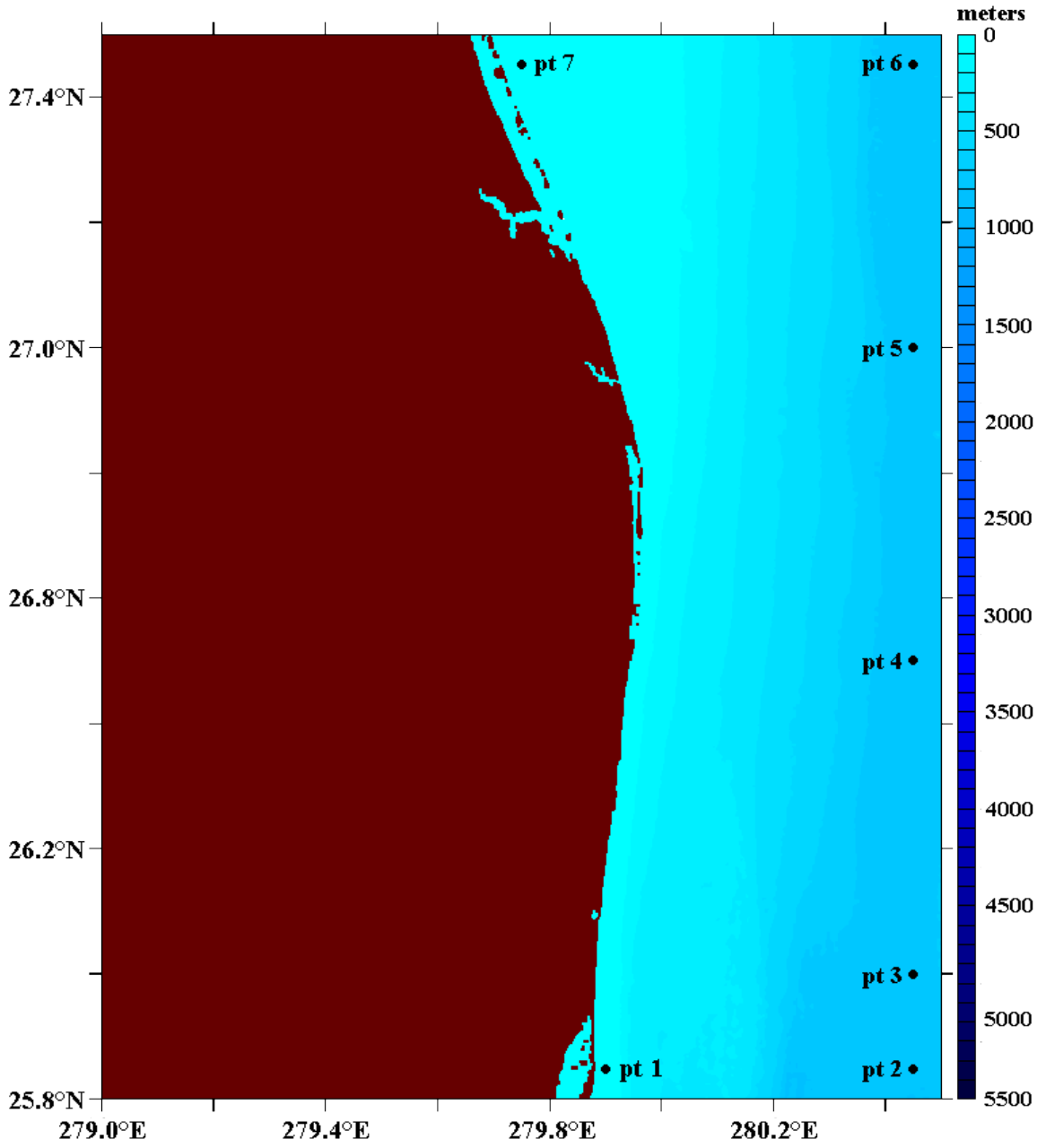

Figure 8. Location of points where time series are compared for testing different domain sizes (see Figure 7).

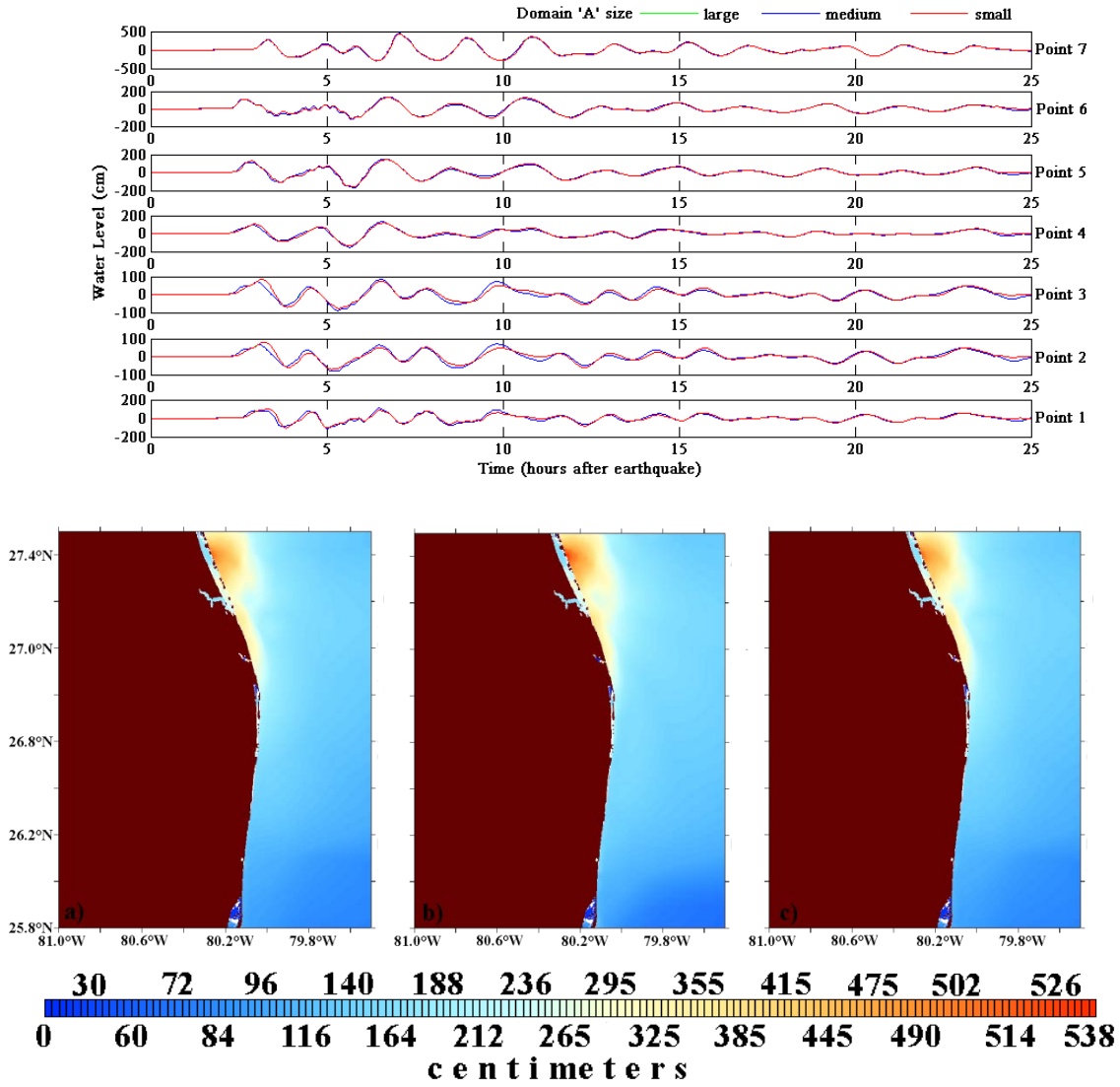

Figure 9. Comparison of time series plots (top) and maximum tsunami wave amplitude distribution. The bottom plots of large domain (a) and medium domain (b) are adjusted to match that of the small domain (c) for consistency.

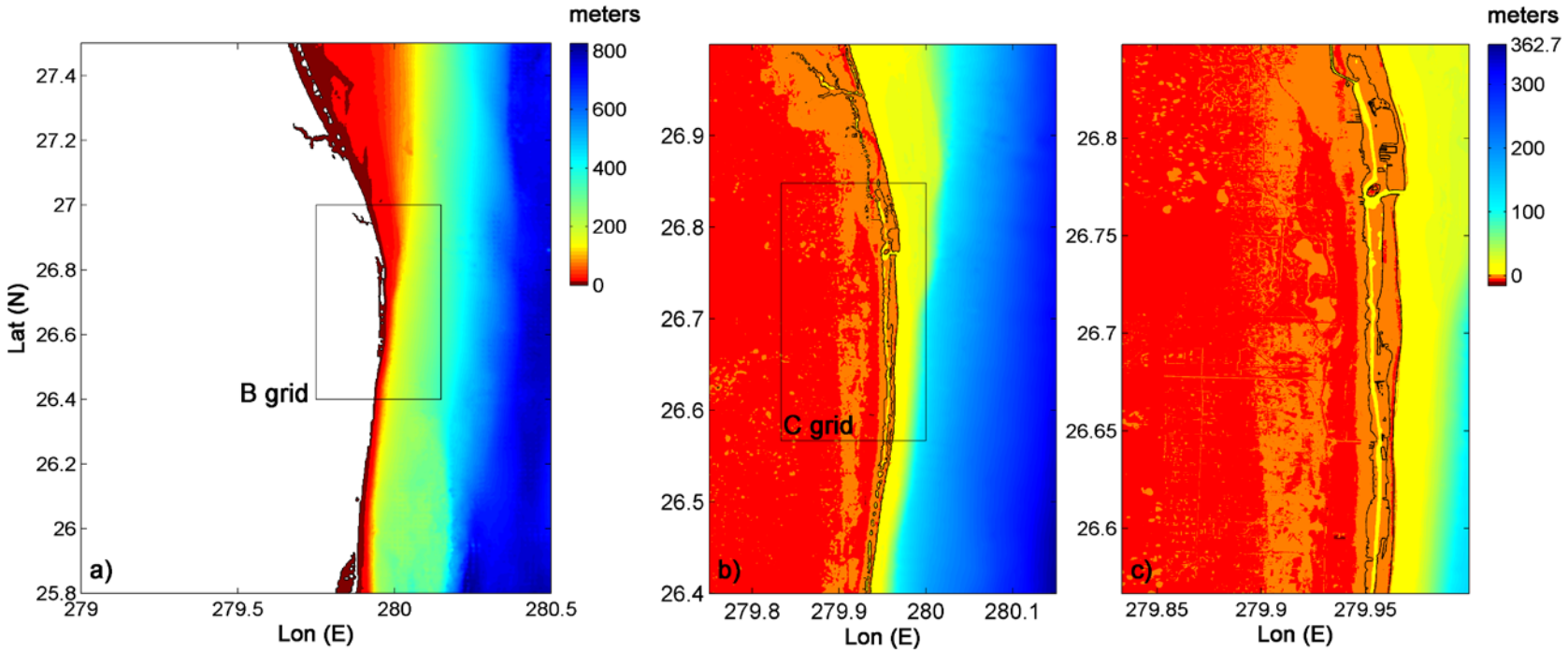

Figure 10. Plot of DEM extents used for both the high-resolution reference model and forecast model. a) A grid with the box indicating the extent of B grid; b) B grid with the box indicating the extent of C grid; c) C grid. Grid resolutions used are indicated in Table 1.

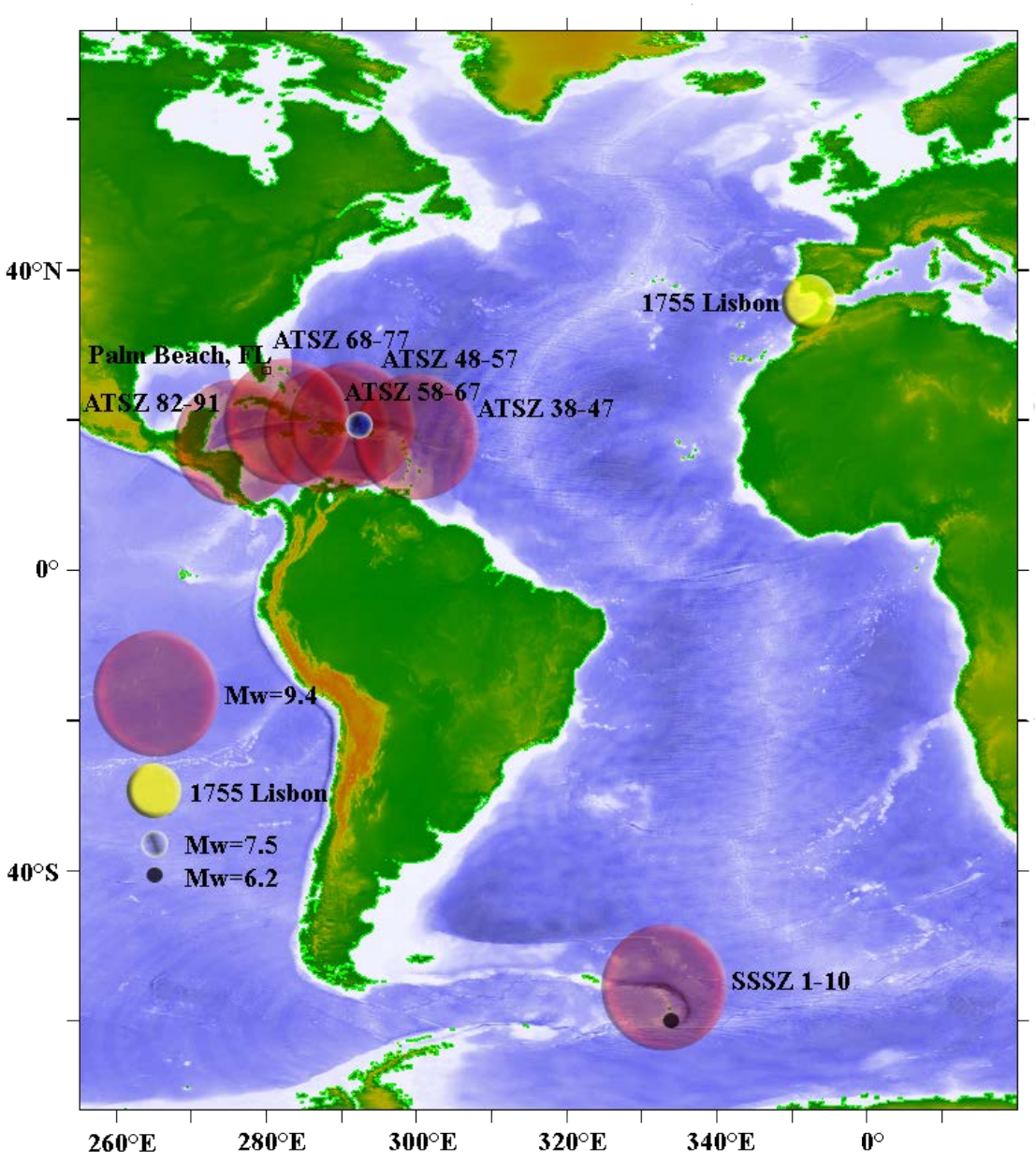

Figure 11. Plot locating the scenarios (Mw=9.4, Mw=7.5, Mw=6.2, and 1755 Lisbon) used for testing the stability and reliability of the forecast and reference models in relation to the location of Palm Beach, Florida.

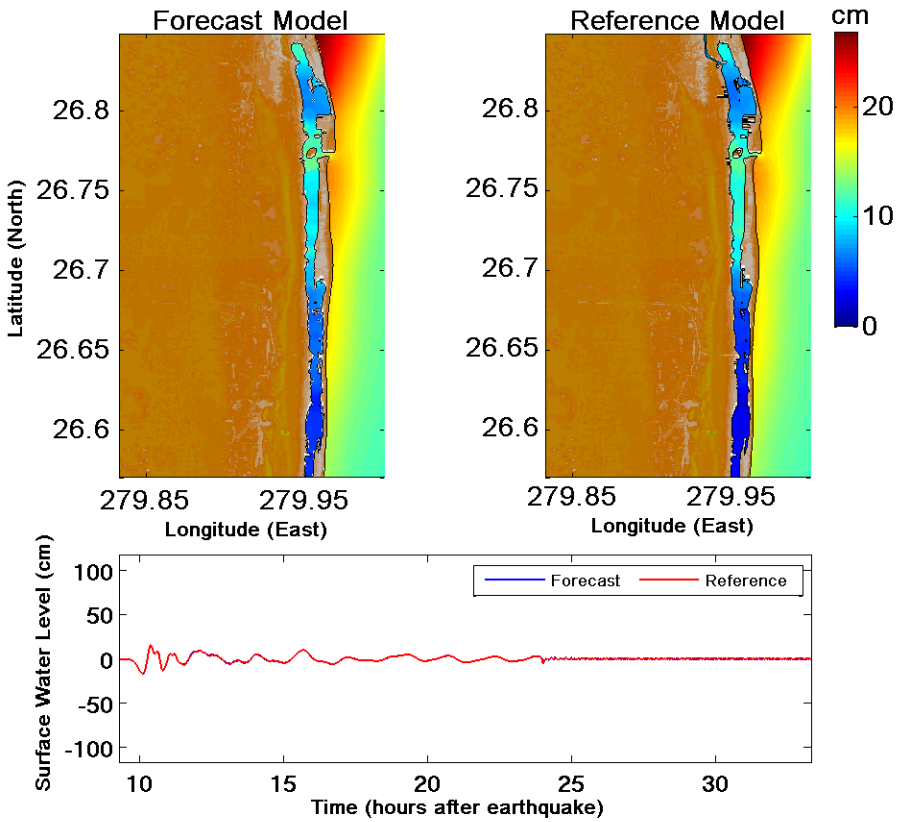

Figure 12. Plot of maximum tsunami wave amplitude distribution (top) and time series (bottom) at Lake Worth Pier tide gauge for the 1755 Lisbon tsunami.

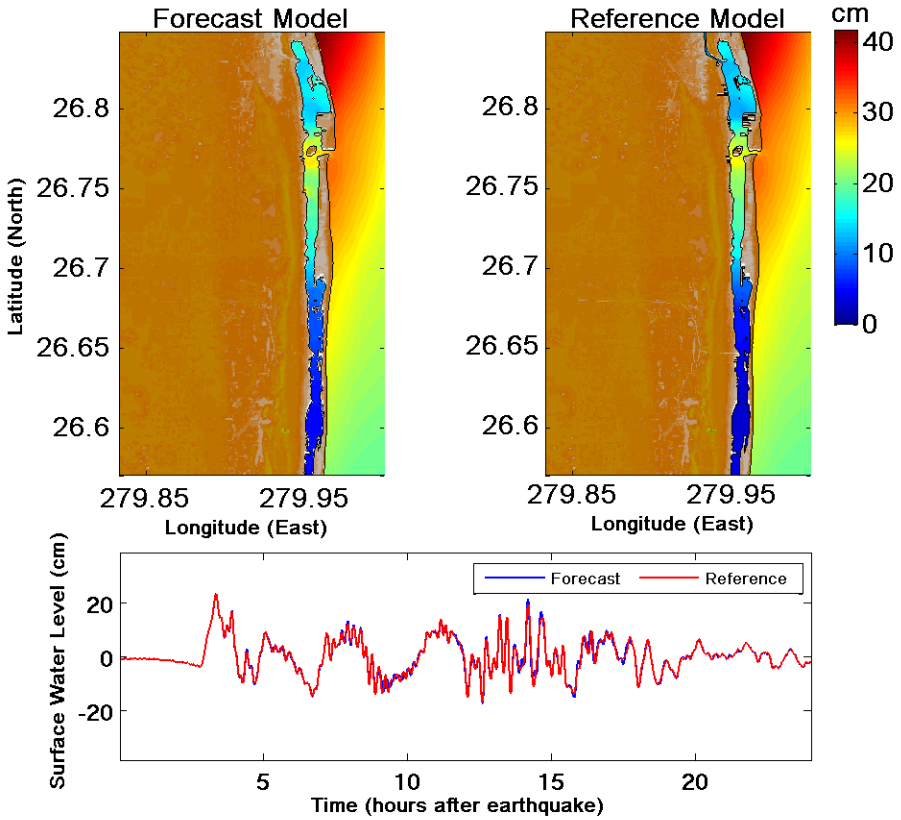

Figure 13. Plot of maximum tsunami wave amplitude distribution (top) and time series (bottom) at Lake Worth Pier tide gauge for the mega-tsunami event ATSZ 38-47.

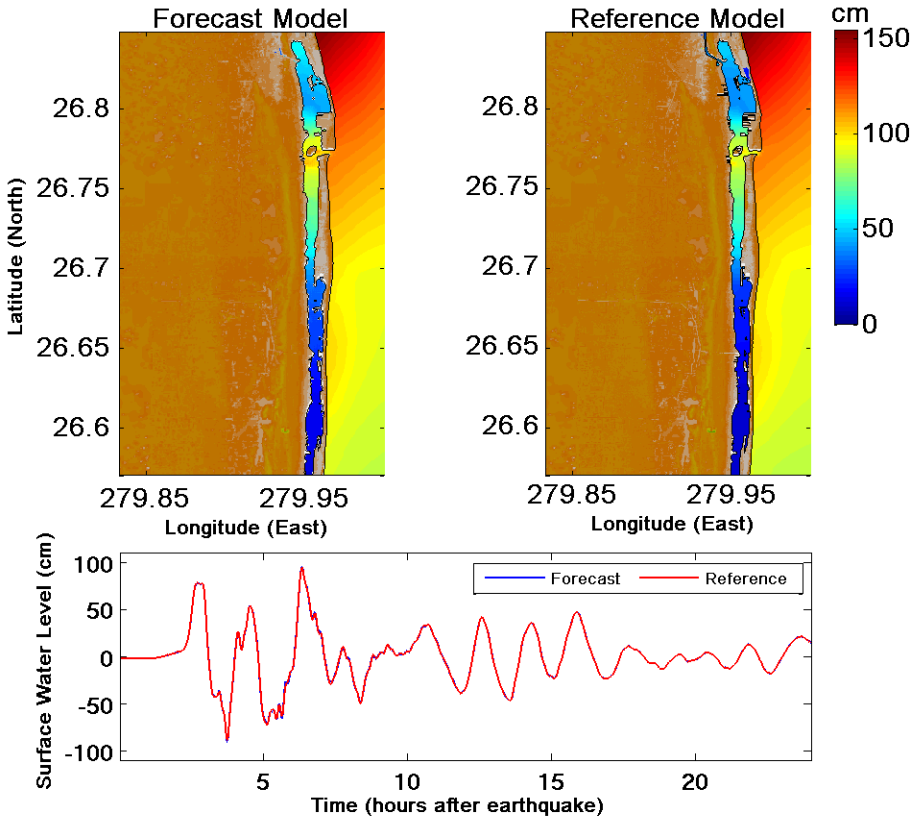

Figure 14. Plot of maximum tsunami wave amplitude distribution (top) and time series (bottom) at Lake Worth Pier tide gauge for the mega-tsunami event ATSZ 48-57.

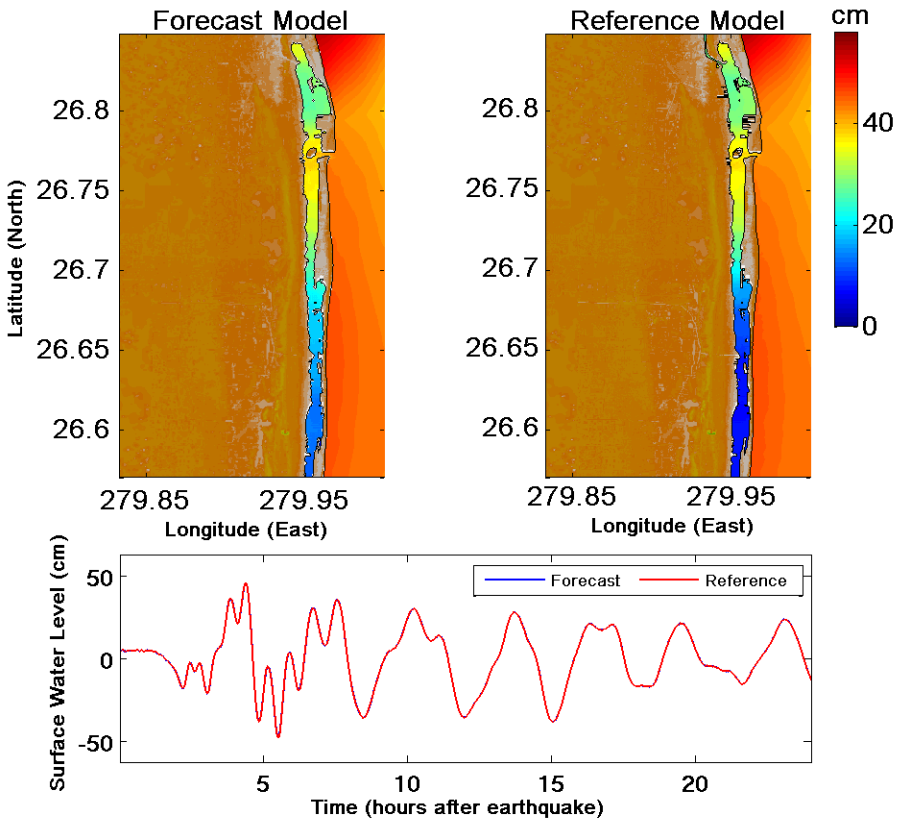

Figure 15. Plot of maximum tsunami wave amplitude distribution (top) and time series (bottom) at Lake Worth Pier tide gauge for the mega-tsunami event ATSZ 58-67.

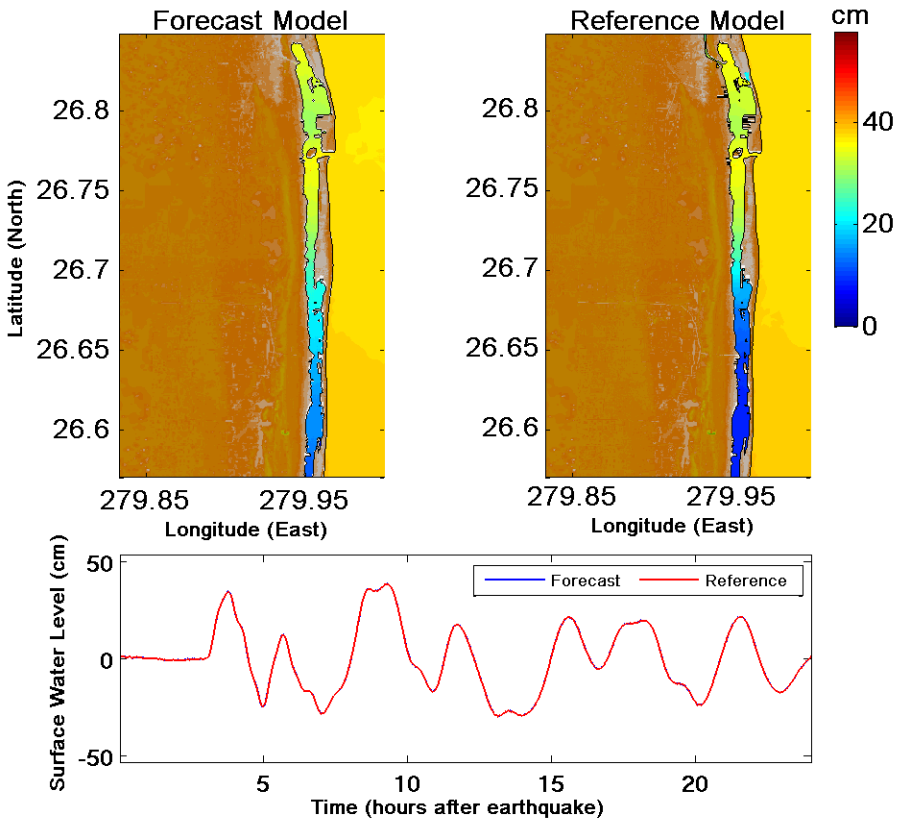

Figure 16. Plot of maximum tsunami wave amplitude distribution (top) and time series (bottom) at Lake Worth Pier tide gauge for the mega-tsunami event ATSZ 68-77.

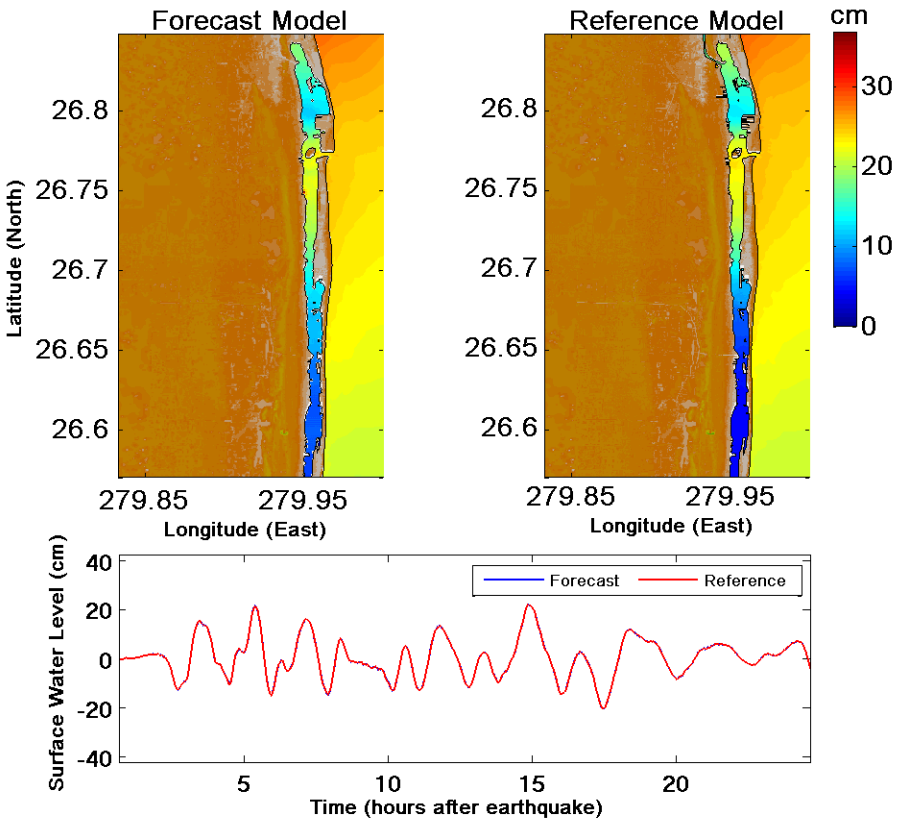

Figure 17. Plot of maximum tsunami wave amplitude distribution (top) and time series (bottom) at Lake Worth Pier tide gauge for the mega-tsunami event ATSZ 82-91.

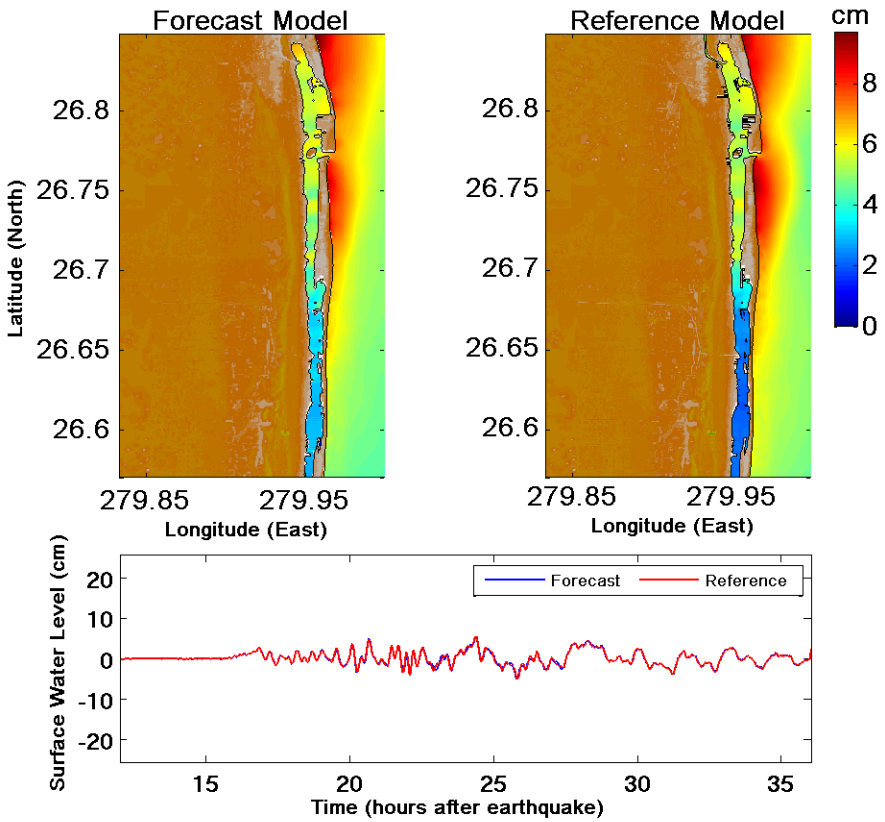

Figure 18. Plot of maximum tsunami wave amplitude distribution (top) and time series (bottom) at Lake Worth Pier tide gauge for the mega-tsunami event SSSZ 1-10.

Figure 19. Google map plot of northern part of Singer Island showing the water passageway.

Appendix A. MOST code *.in file

Development of the Palm Beach, Florida, tsunami forecast model occurred prior to parameter changes that were made to reflect modifications to the MOST model code. As a result, the input file for running both the optimized tsunami forecast model and the high-resolution reference inundation model in MOST have been updated accordingly. Appendix A1 and A2 provide the updated files for Palm Beach.

A1. Reference model *.in file for Palm Beach, Florida

0.0001	Minimum amplitude of input offshore wave (m)
1	Input minimum depth for offshore (m)
0.1	Input "dry land" depth for inundation (m)
0.0009	Input friction coefficient (n**2)
1	A & B-grid runup flag (0=disallow, 1=allow runup)
300.0	Blow-up limit (maximum eta before blow-up)
0.4	Input time step (sec)
72000	Input number of steps
5	Compute "A" arrays every n^{th} time step, n=
5	Compute "B" arrays every n^{th} time step, n=
150	Input number of steps between snapshots
0	...Starting from
1	...Saving grid every n^{th} node, n=1

A2. Forecast model *.in file for Palm Beach, Florida

0.0001	Minimum amplitude of input offshore wave (m)
1	Input minimum depth for offshore (m)
0.1	Input "dry land" depth for inundation (m)
0.0009	Input friction coefficient (n**2)
1	A & B-grid runup flag (0=disallow, 1=allow runup)
300.0	Blow-up limit (maximum eta before blow-up)
1.0	Input time step (sec)
28800	Input number of steps
4	Compute "A" arrays every n^{th} time step, n=
4	Compute "B" arrays every n^{th} time step, n=
60	Input number of steps between snapshots
0	...Starting from
1	...Saving grid every n^{th} node, n=1

Appendix B. Propagation Database: Atlantic Ocean Unit Sources

This section lists the earthquake parameters of each unit source in the Atlantic Ocean which covers the Caribbean and South Sandwich sources as of 30 January 2013. The development of the Palm Beach, Florida, forecast model was done early 2011 thus using an earlier version of the unit sources.

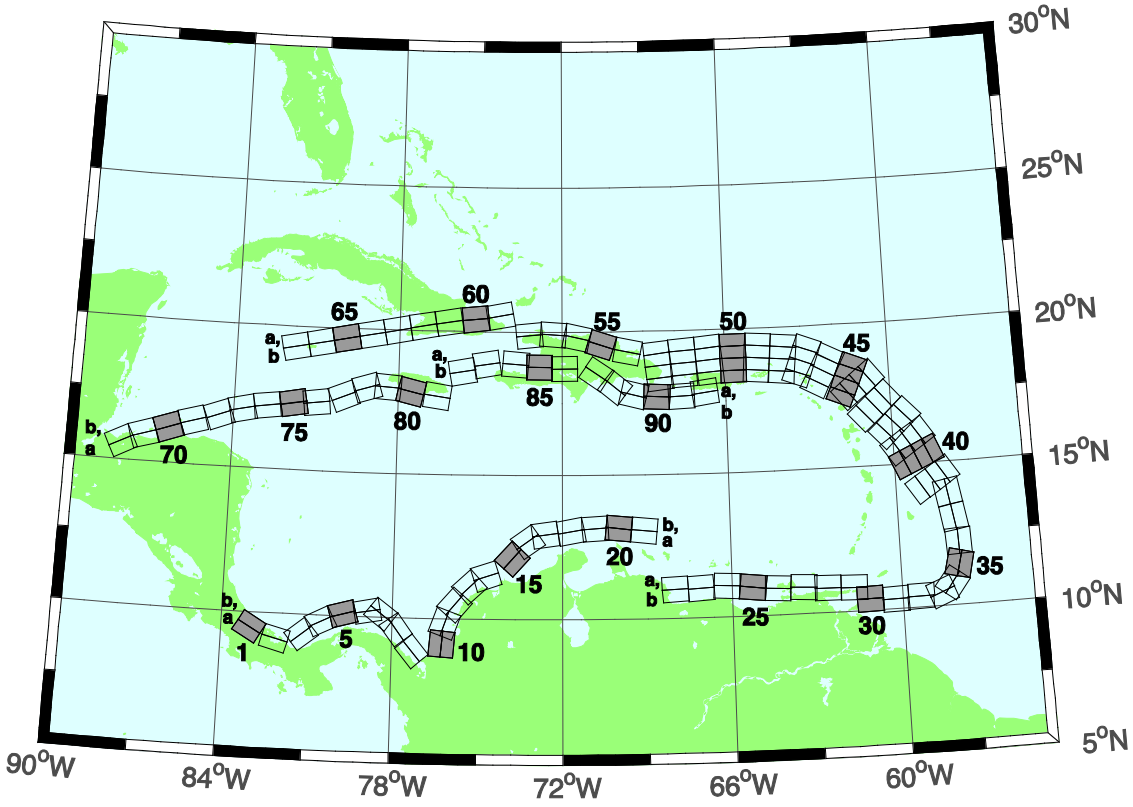

Figure B.1. Atlantic Source Zone unit sources

Table B.1. Earthquake parameter for unit sources in Atlantic.

Unit Source	Description	Lon (°)	Lat (°)	Strike (°)	Dip (°)	Depth (km)
atsz-01a	Atlantic Source Zone	-83.2020	9.1449	27.50	120.00	28.09
atsz-01b	Atlantic Source Zone	-83.0000	9.4899	27.50	120.00	5.00
atsz-02a	Atlantic Source Zone	-82.1932	8.7408	27.50	105.11	28.09
atsz-02b	Atlantic Source Zone	-82.0880	9.1254	27.50	105.11	5.00
atsz-03a	Atlantic Source Zone	-80.9172	9.0103	30.00	51.31	30.00
atsz-03b	Atlantic Source Zone	-81.1636	9.3139	30.00	51.31	5.00
atsz-04a	Atlantic Source Zone	-80.3265	9.4308	30.00	63.49	30.00
atsz-04b	Atlantic Source Zone	-80.5027	9.7789	30.00	63.49	5.00
atsz-05a	Atlantic Source Zone	-79.6247	9.6961	30.00	74.44	30.00
atsz-05b	Atlantic Source Zone	-79.7307	10.0708	30.00	74.44	5.00
atsz-06a	Atlantic Source Zone	-78.8069	9.8083	30.00	79.71	30.00
atsz-06b	Atlantic Source Zone	-78.8775	10.1910	30.00	79.71	5.00
atsz-07a	Atlantic Source Zone	-78.6237	9.7963	30.00	127.25	30.00
atsz-07b	Atlantic Source Zone	-78.3845	10.1059	30.00	127.25	5.00
atsz-08a	Atlantic Source Zone	-78.1693	9.3544	30.00	143.76	30.00
atsz-08b	Atlantic Source Zone	-77.8511	9.5844	30.00	143.76	5.00
atsz-09a	Atlantic Source Zone	-77.5913	8.5989	30.00	139.93	30.00
atsz-09b	Atlantic Source Zone	-77.2900	8.8493	30.00	139.93	5.00
atsz-10a	Atlantic Source Zone	-75.8109	9.0881	17.00	4.67	19.62
atsz-10b	Atlantic Source Zone	-76.2445	9.1231	17.00	4.67	5.00
atsz-11a	Atlantic Source Zone	-75.7406	9.6929	17.00	19.67	19.62
atsz-11b	Atlantic Source Zone	-76.1511	9.8375	17.00	19.67	5.00
atsz-12a	Atlantic Source Zone	-75.4763	10.2042	17.00	40.40	19.62
atsz-12b	Atlantic Source Zone	-75.8089	10.4826	17.00	40.40	5.00
atsz-13a	Atlantic Source Zone	-74.9914	10.7914	17.00	47.17	19.62
atsz-13b	Atlantic Source Zone	-75.2890	11.1064	17.00	47.17	5.00
atsz-14a	Atlantic Source Zone	-74.5666	11.0708	17.00	71.68	19.62
atsz-14b	Atlantic Source Zone	-74.7043	11.4786	17.00	71.68	5.00
atsz-15a	Atlantic Source Zone	-73.4576	11.8012	17.00	42.69	19.62
atsz-15b	Atlantic Source Zone	-73.7805	12.0924	17.00	42.69	5.00
atsz-16a	Atlantic Source Zone	-72.9788	12.3365	17.00	54.75	19.62
atsz-16b	Atlantic Source Zone	-73.2329	12.6873	17.00	54.75	5.00
atsz-17a	Atlantic Source Zone	-72.5454	12.5061	17.00	81.96	19.62
atsz-17b	Atlantic Source Zone	-72.6071	12.9314	17.00	81.96	5.00
atsz-18a	Atlantic Source Zone	-71.6045	12.6174	17.00	79.63	19.62
atsz-18b	Atlantic Source Zone	-71.6839	13.0399	17.00	79.63	5.00
atsz-19a	Atlantic Source Zone	-70.7970	12.7078	17.00	86.32	19.62
atsz-19b	Atlantic Source Zone	-70.8253	13.1364	17.00	86.32	5.00

Table B.1 (continued). Earthquake parameter for unit sources in Atlantic.

atsz-20a	Atlantic Source Zone	-70.0246	12.7185	17.00	95.94	19.62
atsz-20b	Atlantic Source Zone	-69.9789	13.1457	17.00	95.94	5.00
atsz-21a	Atlantic Source Zone	-69.1244	12.6320	17.00	95.94	19.62
atsz-21b	Atlantic Source Zone	-69.0788	13.0592	17.00	95.94	5.00
atsz-22a	Atlantic Source Zone	-68.0338	11.4286	15.00	266.94	17.94
atsz-22b	Atlantic Source Zone	-68.0102	10.9954	15.00	266.94	5.00
atsz-23a	Atlantic Source Zone	-67.1246	11.4487	15.00	266.94	17.94
atsz-23b	Atlantic Source Zone	-67.1010	11.0155	15.00	266.94	5.00
atsz-24a	Atlantic Source Zone	-66.1656	11.5055	15.00	273.30	17.94
atsz-24b	Atlantic Source Zone	-66.1911	11.0724	15.00	273.30	5.00
atsz-25a	Atlantic Source Zone	-65.2126	11.4246	15.00	276.36	17.94
atsz-25b	Atlantic Source Zone	-65.2616	10.9934	15.00	276.36	5.00
atsz-26a	Atlantic Source Zone	-64.3641	11.3516	15.00	272.87	17.94
atsz-26b	Atlantic Source Zone	-64.3862	10.9183	15.00	272.87	5.00
atsz-27a	Atlantic Source Zone	-63.4472	11.3516	15.00	272.93	17.94
atsz-27b	Atlantic Source Zone	-63.4698	10.9183	15.00	272.93	5.00
atsz-28a	Atlantic Source Zone	-62.6104	11.2831	15.00	271.11	17.94
atsz-28b	Atlantic Source Zone	-62.6189	10.8493	15.00	271.11	5.00
atsz-29a	Atlantic Source Zone	-61.6826	11.2518	15.00	271.57	17.94
atsz-29b	Atlantic Source Zone	-61.6947	10.8181	15.00	271.57	5.00
atsz-30a	Atlantic Source Zone	-61.1569	10.8303	15.00	269.01	17.94
atsz-30b	Atlantic Source Zone	-61.1493	10.3965	15.00	269.01	5.00
atsz-31a	Atlantic Source Zone	-60.2529	10.7739	15.00	269.01	17.94
atsz-31b	Atlantic Source Zone	-60.2453	10.3401	15.00	269.01	5.00
atsz-32a	Atlantic Source Zone	-59.3510	10.8123	15.00	269.01	17.94
atsz-32b	Atlantic Source Zone	-59.3734	10.3785	15.00	269.01	5.00
atsz-33a	Atlantic Source Zone	-58.7592	10.8785	15.00	248.62	17.94
atsz-33b	Atlantic Source Zone	-58.5984	10.4745	15.00	248.62	5.00
atsz-34a	Atlantic Source Zone	-58.5699	11.0330	15.00	217.15	17.94
atsz-34b	Atlantic Source Zone	-58.2179	10.7710	15.00	217.15	5.00
atsz-35a	Atlantic Source Zone	-58.3549	11.5300	15.00	193.68	17.94
atsz-35b	Atlantic Source Zone	-57.9248	11.4274	15.00	193.68	5.00
atsz-36a	Atlantic Source Zone	-58.3432	12.1858	15.00	177.65	17.94
atsz-36b	Atlantic Source Zone	-57.8997	12.2036	15.00	177.65	5.00
atsz-37a	Atlantic Source Zone	-58.4490	12.9725	15.00	170.73	17.94
atsz-37b	Atlantic Source Zone	-58.0095	13.0424	15.00	170.73	5.00
atsz-38a	Atlantic Source Zone	-58.6079	13.8503	15.00	170.22	17.94
atsz-38b	Atlantic Source Zone	-58.1674	13.9240	15.00	170.22	5.00
atsz-39a	Atlantic Source Zone	-58.6667	14.3915	15.00	146.85	17.94
atsz-39b	Atlantic Source Zone	-58.2913	14.6287	15.00	146.85	5.00

Table B.1 (continued). Earthquake parameter for unit sources in Atlantic.

atsz-39y	Atlantic Source Zone	-59.4168	13.9171	15.00	146.85	43.82
atsz-39z	Atlantic Source Zone	-59.0415	14.1543	15.00	146.85	30.88
atsz-40a	Atlantic Source Zone	-59.1899	15.2143	15.00	156.23	17.94
atsz-40b	Atlantic Source Zone	-58.7781	15.3892	15.00	156.23	5.00
atsz-40y	Atlantic Source Zone	-60.0131	14.8646	15.00	156.23	43.82
atsz-40z	Atlantic Source Zone	-59.6012	15.0395	15.00	156.23	30.88
atsz-41a	Atlantic Source Zone	-59.4723	15.7987	15.00	146.33	17.94
atsz-41b	Atlantic Source Zone	-59.0966	16.0392	15.00	146.33	5.00
atsz-41y	Atlantic Source Zone	-60.2229	15.3177	15.00	146.33	43.82
atsz-41z	Atlantic Source Zone	-59.8473	15.5582	15.00	146.33	30.88
atsz-42a	Atlantic Source Zone	-59.9029	16.4535	15.00	136.99	17.94
atsz-42b	Atlantic Source Zone	-59.5716	16.7494	15.00	136.99	5.00
atsz-42y	Atlantic Source Zone	-60.5645	15.8616	15.00	136.99	43.82
atsz-42z	Atlantic Source Zone	-60.2334	16.1575	15.00	136.99	30.88
atsz-43a	Atlantic Source Zone	-60.5996	17.0903	15.00	138.71	17.94
atsz-43b	Atlantic Source Zone	-60.2580	17.3766	15.00	138.71	5.00
atsz-43y	Atlantic Source Zone	-61.2818	16.5177	15.00	138.71	43.82
atsz-43z	Atlantic Source Zone	-60.9404	16.8040	15.00	138.71	30.88
atsz-44a	Atlantic Source Zone	-61.1559	17.8560	15.00	141.07	17.94
atsz-44b	Atlantic Source Zone	-60.8008	18.1286	15.00	141.07	5.00
atsz-44y	Atlantic Source Zone	-61.8651	17.3108	15.00	141.07	43.82
atsz-44z	Atlantic Source Zone	-61.5102	17.5834	15.00	141.07	30.88
atsz-45a	Atlantic Source Zone	-61.5491	18.0566	15.00	112.84	17.94
atsz-45b	Atlantic Source Zone	-61.3716	18.4564	15.00	112.84	5.00
atsz-45y	Atlantic Source Zone	-61.9037	17.2569	15.00	112.84	43.82
atsz-45z	Atlantic Source Zone	-61.7260	17.6567	15.00	112.84	30.88
atsz-46a	Atlantic Source Zone	-62.4217	18.4149	15.00	117.86	17.94
atsz-46b	Atlantic Source Zone	-62.2075	18.7985	15.00	117.86	5.00
atsz-46y	Atlantic Source Zone	-62.8493	17.6477	15.00	117.86	43.82
atsz-46z	Atlantic Source Zone	-62.6352	18.0313	15.00	117.86	30.88
atsz-47a	Atlantic Source Zone	-63.1649	18.7844	20.00	110.46	22.10
atsz-47b	Atlantic Source Zone	-63.0087	19.1798	20.00	110.46	5.00
atsz-47y	Atlantic Source Zone	-63.4770	17.9936	20.00	110.46	56.30
atsz-47z	Atlantic Source Zone	-63.3205	18.3890	20.00	110.46	39.20
atsz-48a	Atlantic Source Zone	-63.8800	18.8870	20.00	95.37	22.10
atsz-48b	Atlantic Source Zone	-63.8382	19.3072	20.00	95.37	5.00
atsz-48y	Atlantic Source Zone	-63.9643	18.0465	20.00	95.37	56.30
atsz-48z	Atlantic Source Zone	-63.9216	18.4667	20.00	95.37	39.20
atsz-49a	Atlantic Source Zone	-64.8153	18.9650	20.00	94.34	22.10
atsz-49b	Atlantic Source Zone	-64.7814	19.3859	20.00	94.34	5.00

Table B.1 (continued). Earthquake parameter for unit sources in Atlantic.

atsz-49y	Atlantic Source Zone	-64.8840	18.1233	20.00	94.34	56.30
atsz-49z	Atlantic Source Zone	-64.8492	18.5442	20.00	94.34	39.20
atsz-50a	Atlantic Source Zone	-65.6921	18.9848	20.00	89.59	22.10
atsz-50b	Atlantic Source Zone	-65.6953	19.4069	20.00	89.59	5.00
atsz-50y	Atlantic Source Zone	-65.6874	18.1407	20.00	89.59	56.30
atsz-50z	Atlantic Source Zone	-65.6887	18.5628	20.00	89.59	39.20
atsz-51a	Atlantic Source Zone	-66.5742	18.9484	20.00	84.98	22.10
atsz-51b	Atlantic Source Zone	-66.6133	19.3688	20.00	84.98	5.00
atsz-51y	Atlantic Source Zone	-66.4977	18.1076	20.00	84.98	56.30
atsz-51z	Atlantic Source Zone	-66.5353	18.5280	20.00	84.98	39.20
atsz-52a	Atlantic Source Zone	-67.5412	18.8738	20.00	85.87	22.10
atsz-52b	Atlantic Source Zone	-67.5734	19.2948	20.00	85.87	5.00
atsz-52y	Atlantic Source Zone	-67.4781	18.0319	20.00	85.87	56.30
atsz-52z	Atlantic Source Zone	-67.5090	18.4529	20.00	85.87	39.20
atsz-53a	Atlantic Source Zone	-68.4547	18.7853	20.00	83.64	22.10
atsz-53b	Atlantic Source Zone	-68.5042	19.2048	20.00	83.64	5.00
atsz-53y	Atlantic Source Zone	-68.3575	17.9463	20.00	83.64	56.30
atsz-53z	Atlantic Source Zone	-68.4055	18.3658	20.00	83.64	39.20
atsz-54a	Atlantic Source Zone	-69.6740	18.8841	20.00	101.54	22.10
atsz-54b	Atlantic Source Zone	-69.5846	19.2976	20.00	101.54	5.00
atsz-55a	Atlantic Source Zone	-70.7045	19.1376	20.00	108.19	22.10
atsz-55b	Atlantic Source Zone	-70.5647	19.5386	20.00	108.19	5.00
atsz-56a	Atlantic Source Zone	-71.5368	19.3853	20.00	102.64	22.10
atsz-56b	Atlantic Source Zone	-71.4386	19.7971	20.00	102.64	5.00
atsz-57a	Atlantic Source Zone	-72.3535	19.4838	20.00	94.20	22.10
atsz-57b	Atlantic Source Zone	-72.3206	19.9047	20.00	94.20	5.00
atsz-58a	Atlantic Source Zone	-73.1580	19.4498	20.00	84.34	22.10
atsz-58b	Atlantic Source Zone	-73.2022	19.8698	20.00	84.34	5.00
atsz-59a	Atlantic Source Zone	-74.3567	20.9620	20.00	259.74	22.10
atsz-59b	Atlantic Source Zone	-74.2764	20.5467	20.00	259.74	5.00
atsz-60a	Atlantic Source Zone	-75.2386	20.8622	15.00	264.18	17.94
atsz-60b	Atlantic Source Zone	-75.1917	20.4306	15.00	264.18	5.00
atsz-61a	Atlantic Source Zone	-76.2383	20.7425	15.00	260.70	17.94
atsz-61b	Atlantic Source Zone	-76.1635	20.3144	15.00	260.70	5.00
atsz-62a	Atlantic Source Zone	-77.2021	20.5910	15.00	259.95	17.94
atsz-62b	Atlantic Source Zone	-77.1214	20.1638	15.00	259.95	5.00
atsz-63a	Atlantic Source Zone	-78.1540	20.4189	15.00	259.03	17.94
atsz-63b	Atlantic Source Zone	-78.0661	19.9930	15.00	259.03	5.00
atsz-64a	Atlantic Source Zone	-79.0959	20.2498	15.00	259.24	17.94
atsz-64b	Atlantic Source Zone	-79.0098	19.8236	15.00	259.24	5.00

Table B.1 (continued). Earthquake parameter for unit sources in Atlantic.

atsz-65a	Atlantic Source Zone	-80.0393	20.0773	15.00	258.85	17.94
atsz-65b	Atlantic Source Zone	-79.9502	19.6516	15.00	258.85	5.00
atsz-66a	Atlantic Source Zone	-80.9675	19.8993	15.00	258.60	17.94
atsz-66b	Atlantic Source Zone	-80.8766	19.4740	15.00	258.60	5.00
atsz-67a	Atlantic Source Zone	-81.9065	19.7214	15.00	258.51	17.94
atsz-67b	Atlantic Source Zone	-81.8149	19.2962	15.00	258.51	5.00
atsz-68a	Atlantic Source Zone	-87.8003	15.2509	15.00	62.69	17.94
atsz-68b	Atlantic Source Zone	-88.0070	15.6364	15.00	62.69	5.00
atsz-69a	Atlantic Source Zone	-87.0824	15.5331	15.00	72.73	17.94
atsz-69b	Atlantic Source Zone	-87.2163	15.9474	15.00	72.73	5.00
atsz-70a	Atlantic Source Zone	-86.1622	15.8274	15.00	70.64	17.94
atsz-70b	Atlantic Source Zone	-86.3120	16.2367	15.00	70.64	5.00
atsz-71a	Atlantic Source Zone	-85.3117	16.1052	15.00	73.70	17.94
atsz-71b	Atlantic Source Zone	-85.4387	16.5216	15.00	73.70	5.00
atsz-72a	Atlantic Source Zone	-84.3470	16.3820	15.00	69.66	17.94
atsz-72b	Atlantic Source Zone	-84.5045	16.7888	15.00	69.66	5.00
atsz-73a	Atlantic Source Zone	-83.5657	16.6196	15.00	77.36	17.94
atsz-73b	Atlantic Source Zone	-83.6650	17.0429	15.00	77.36	5.00
atsz-74a	Atlantic Source Zone	-82.7104	16.7695	15.00	82.35	17.94
atsz-74b	Atlantic Source Zone	-82.7709	17.1995	15.00	82.35	5.00
atsz-75a	Atlantic Source Zone	-81.7297	16.9003	15.00	79.86	17.94
atsz-75b	Atlantic Source Zone	-81.8097	17.3274	15.00	79.86	5.00
atsz-76a	Atlantic Source Zone	-80.9196	16.9495	15.00	82.95	17.94
atsz-76b	Atlantic Source Zone	-80.9754	17.3801	15.00	82.95	5.00
atsz-77a	Atlantic Source Zone	-79.8086	17.2357	15.00	67.95	17.94
atsz-77b	Atlantic Source Zone	-79.9795	17.6378	15.00	67.95	5.00
atsz-78a	Atlantic Source Zone	-79.0245	17.5415	15.00	73.61	17.94
atsz-78b	Atlantic Source Zone	-79.1532	17.9577	15.00	73.61	5.00
atsz-79a	Atlantic Source Zone	-78.4122	17.5689	15.00	94.07	17.94
atsz-79b	Atlantic Source Zone	-78.3798	18.0017	15.00	94.07	5.00
atsz-80a	Atlantic Source Zone	-77.6403	17.4391	15.00	103.33	17.94
atsz-80b	Atlantic Source Zone	-77.5352	17.8613	15.00	103.33	5.00
atsz-81a	Atlantic Source Zone	-76.6376	17.2984	15.00	98.21	17.94
atsz-81b	Atlantic Source Zone	-76.5726	17.7278	15.00	98.21	5.00
atsz-82a	Atlantic Source Zone	-75.7299	19.0217	15.00	260.15	17.94
atsz-82b	Atlantic Source Zone	-75.6516	18.5942	15.00	260.15	5.00
atsz-83a	Atlantic Source Zone	-74.8351	19.2911	15.00	260.83	17.94
atsz-83b	Atlantic Source Zone	-74.7621	18.8628	15.00	260.83	5.00
atsz-84a	Atlantic Source Zone	-73.6639	19.2991	15.00	274.84	17.94
atsz-84b	Atlantic Source Zone	-73.7026	18.8668	15.00	274.84	5.00

Table B.1 (continued). Earthquake parameter for unit sources in Atlantic.

atsz-85a	Atlantic Source Zone	-72.8198	19.2019	15.00	270.60	17.94
atsz-85b	Atlantic Source Zone	-72.8246	18.7681	15.00	270.60	5.00
atsz-86a	Atlantic Source Zone	-71.9143	19.1477	15.00	269.06	17.94
atsz-86b	Atlantic Source Zone	-71.9068	18.7139	15.00	269.06	5.00
atsz-87a	Atlantic Source Zone	-70.4738	18.8821	15.00	304.49	17.94
atsz-87b	Atlantic Source Zone	-70.7329	18.5245	15.00	304.49	5.00
atsz-88a	Atlantic Source Zone	-69.7710	18.3902	15.00	308.94	17.94
atsz-88b	Atlantic Source Zone	-70.0547	18.0504	15.00	308.44	5.00
atsz-89a	Atlantic Source Zone	-69.2635	18.2099	15.00	283.88	17.94
atsz-89b	Atlantic Source Zone	-69.3728	17.7887	15.00	283.88	5.00
atsz-90a	Atlantic Source Zone	-68.5059	18.1443	15.00	272.93	17.94
atsz-90b	Atlantic Source Zone	-68.5284	17.7110	15.00	272.93	5.00
atsz-91a	Atlantic Source Zone	-67.6428	18.1438	15.00	267.84	17.94
atsz-91b	Atlantic Source Zone	-67.6256	17.7103	15.00	267.84	5.00
atsz-92a	Atlantic Source Zone	-66.8261	18.2536	15.00	262.00	17.94
atsz-92b	Atlantic Source Zone	-66.7627	17.8240	15.00	262.00	5.00

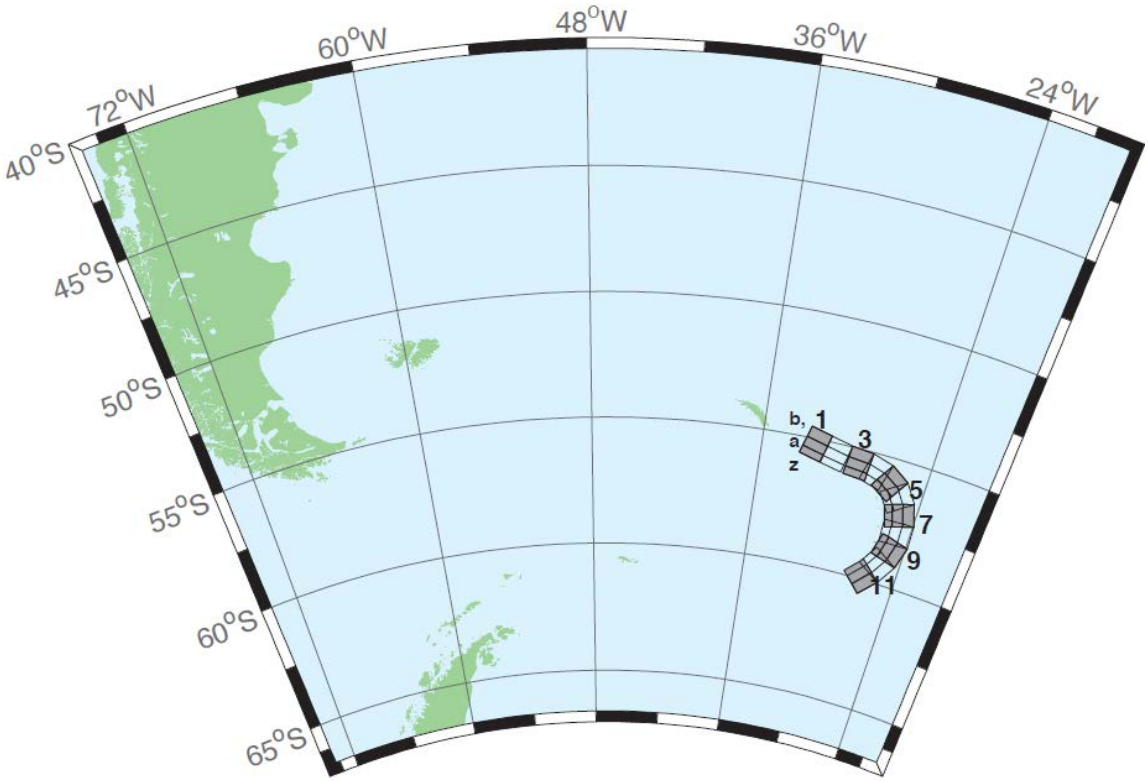

Figure B.2. South Sandwich Source Zone unit sources

Table B.2. Earthquake parameters for unit sources in South Sandwich.

sssz-01a	South Sandwich Source Zone	-32.3713	-55.4655	28.528	104.6905	17.511
sssz-01b	South Sandwich Source Zone	-32.1953	-55.0832	9.957	104.6905	8.866
sssz-01z	South Sandwich Source Zone	-32.5091	-55.7624	46.989	104.6905	41.391
sssz-02a	South Sandwich Source Zone	-30.8028	-55.6842	28.528	102.4495	17.511
sssz-02b	South Sandwich Source Zone	-30.6524	-55.2982	9.957	102.4495	8.866
sssz-02z	South Sandwich Source Zone	-30.9207	-55.9839	46.989	102.4495	41.391
sssz-03a	South Sandwich Source Zone	-29.0824	-55.8403	28.528	95.5322	17.511
sssz-03b	South Sandwich Source Zone	-29.0149	-55.4469	9.957	95.5322	8.866
sssz-03z	South Sandwich Source Zone	-29.1354	-56.1458	46.989	95.5322	41.391
sssz-04a	South Sandwich Source Zone	-27.8128	-55.9796	28.528	106.1387	17.511
sssz-04b	South Sandwich Source Zone	-27.6174	-55.5999	9.957	106.1387	8.866
sssz-04z	South Sandwich Source Zone	-27.9659	-56.2744	46.989	106.1387	41.391
sssz-05a	South Sandwich Source Zone	-26.7928	-56.2481	28.528	123.1030	17.511
sssz-05b	South Sandwich Source Zone	-26.4059	-55.9170	9.957	123.1030	8.866
sssz-05z	South Sandwich Source Zone	-27.0955	-56.5052	46.989	123.1030	41.391
sssz-06a	South Sandwich Source Zone	-26.1317	-56.6466	23.277	145.6243	16.110
sssz-06b	South Sandwich Source Zone	-25.5131	-56.4133	9.090	145.6243	8.228
sssz-06z	South Sandwich Source Zone	-26.5920	-56.8194	47.151	145.6243	35.869
sssz-07a	South Sandwich Source Zone	-25.6787	-57.2162	21.210	162.9420	14.235
sssz-07b	South Sandwich Source Zone	-24.9394	-57.0932	7.596	162.9420	7.626
sssz-07z	South Sandwich Source Zone	-26.2493	-57.3109	44.159	162.9420	32.324
sssz-08a	South Sandwich Source Zone	-25.5161	-57.8712	20.328	178.2111	15.908
sssz-08b	South Sandwich Source Zone	-24.7233	-57.8580	8.449	178.2111	8.562
sssz-08z	South Sandwich Source Zone	-26.1280	-57.8813	43.649	178.2111	33.278
sssz-09a	South Sandwich Source Zone	-25.6657	-58.5053	25.759	195.3813	15.715
sssz-09b	South Sandwich Source Zone	-24.9168	-58.6128	8.254	195.3813	8.537
sssz-09z	South Sandwich Source Zone	-26.1799	-58.4313	51.691	195.3813	37.444
sssz-10a	South Sandwich Source Zone	-26.1563	-59.1048	32.821	212.5129	15.649
sssz-10b	South Sandwich Source Zone	-25.5335	-59.3080	10.449	212.5129	6.581
sssz-10z	South Sandwich Source Zone	-26.5817	-58.9653	54.773	212.5129	42.750
sssz-11a	South Sandwich Source Zone	-27.0794	-59.6799	33.667	224.2397	15.746
sssz-11b	South Sandwich Source Zone	-26.5460	-59.9412	11.325	224.2397	5.927
sssz-11z	South Sandwich Source Zone	-27.4245	-59.5098	57.190	224.2397	43.464

Appendix C. Forecast Model tests in SIFT system.

An effective forecast model must provide reliable and stable data for several hours of simulation. This is accomplished by testing the forecast model with a set of synthetic tsunami events covering a range of tsunami source locations and magnitudes. Testing is also done with selected historical tsunami events when available.

The purpose of testing the forecast model is three-fold. The first objective is to assure that the results obtained with NOAA's tsunami forecast system, which has been released to the Tsunami Warning Centers for operational use, are similar to those obtained by the researcher during the development of the forecast model. The second objective is to test the forecast model for consistency, accuracy, time efficiency, and quality of results over a range of possible tsunami locations and magnitudes. The third objective is to identify bugs and issues in need of resolution by the researcher who developed the forecast model or by the forecast software development team before the next version release to NOAA's two Tsunami Warning Centers.

Local hardware and software applications are used with tools familiar to the researcher(s) to run the Method of Splitting Tsunami (MOST) model during the forecast model development. The test results presented in this section lend confidence that the model performs as developed and produces the same results when initiated within the forecast application in an operational setting as those produced by the researcher during the forecast model development. The test results assure those who rely on the Palm Beach, Florida, tsunami forecast model that consistent results are produced irrespective of system.

C.1 Testing Procedure

The general procedure for forecast model testing is to run a set of synthetic tsunami scenarios and a selected set of historical tsunami events through the forecast system application and compare the results with those obtained by the researcher during the forecast model development as presented in the Tsunami Forecast Model Report. Specific steps taken to test the model include:

1. Identification of testing scenarios, including the standard set of synthetic events, appropriate historical events, and customized synthetic scenarios that may have been used by the researcher(s) in developing the forecast model.
2. Creation of new events to represent customized synthetic scenarios used by the researcher(s) in developing the forecast model, if any.
3. Submission of test model runs with the forecast system, and export of the results from A, B, and C grids, along with time series.
4. Recording applicable metadata, including the specific version of the forecast system used for testing.

5. Examination of forecast model results for instabilities in both time series and plot results.
6. Comparison of forecast model results obtained through the forecast system with those obtained during the forecast model development.
7. Summarization of results with specific mention of quality, consistency, and time efficiency.
8. Reporting of issues identified to modeler and forecast software development team.
9. Retesting the forecast models in the forecast system when reported issues have been addressed or explained.

Simulation of the synthetic model were tested on a DELL PowerEdge R510 computer equipped with two Xeon E5670 processors at 2.93 GHz, each with 12 MBytes of cache and 32 GB memory. The processors are hex core and support hyper-threading, resulting in the computer performing as a 24 processor core machine. Additionally, the testing computer supports 10 Gigabit Ethernet for fast network connections. This computer configuration is similar or the same as the configurations of the computers installed at the Tsunami Warning Centers so the compute times should only vary slightly.

C.2 Results

The Palm Beach forecast model was tested with SIFT version 3.2 with MOST v2.

The Palm Beach forecast model was tested with three synthetic scenarios. Test results from the forecast system and comparisons with the results obtained during the forecast model development are shown numerically in Table C.1 and graphically in Figures C.1 to C.3. The results show that the forecast model is stable and robust, with consistent and high-quality results across geographically distributed tsunami sources. The model run time (wall-clock time) was 22.62 min for 7.99 hr of simulation time, and 11.32 min for 4.0 hr. This run time is not within the 10 min run time for 4 hr of simulation time and does not satisfy time efficiency requirements. The trade-off for taking more than 10 min to simulate 4 hr of tsunami waves is the grid resolution used and the coverage extent of the forecast model at the C-grid level. Satisfying a 10-min run would require a smaller coverage of the C-grid level or a coarser grid resolution, or a combination of both.

The modeled scenarios were stable for all cases tested, with no instabilities or unphysical high-frequency oscillations, referred to as ‘ringing.’ A 30 m slip was used for synthetic cases during development instead of the standard 25 m slip, so a 30 m slip was also used for direct comparison purposes. The largest modeled height of 95 cm originated from the Atlantic source ATSZ 48–57. The smallest signal of 2.8 cm originated from the South Sandwich source SSSZ 1–10. Direct comparisons of output from the forecast tool with development results demonstrated that the wave patterns were nearly identical. Both the maximum and minimum amplitudes obtained during development of the Palm Beach forecast model were higher than the maximum amplitudes obtained using the tsunami

forecast software. The variance was most significant at ATSZ 48–57, with a difference of 13.2 cm in maximum amplitude, and ATSZ 38–47, with a difference of 8.1 cm in minimum amplitude. This difference is attributed to the updates made to the Atlantic unit sources done sometime after the Palm Beach forecast model was developed.

Table C.1. Table of maximum and minimum amplitudes (cm) at the Palm Beach, Florida, warning point for synthetic and historical events tested using SIFT 3.2 and obtained during development.

Scenario Name	Source Zone	Tsunami Source	α [m]	SIFT Max (cm)	Development Max (cm)	SIFT Min (cm)	Development Min (cm)
Mega-tsunami Scenarios							
ATSZ 38-47	Atlantic	A38-A47, B38-B47	30	22.9	24.2	-14.4	-22.5
ATSZ 48-57	Atlantic	A48-A57, B48-B57	30	95.0	108.2	-89.2	-92.1
SSSZ 1-10	South Sandwich	A1-A10, B1-B10	30	2.8	7.4	-2.0	-5.0

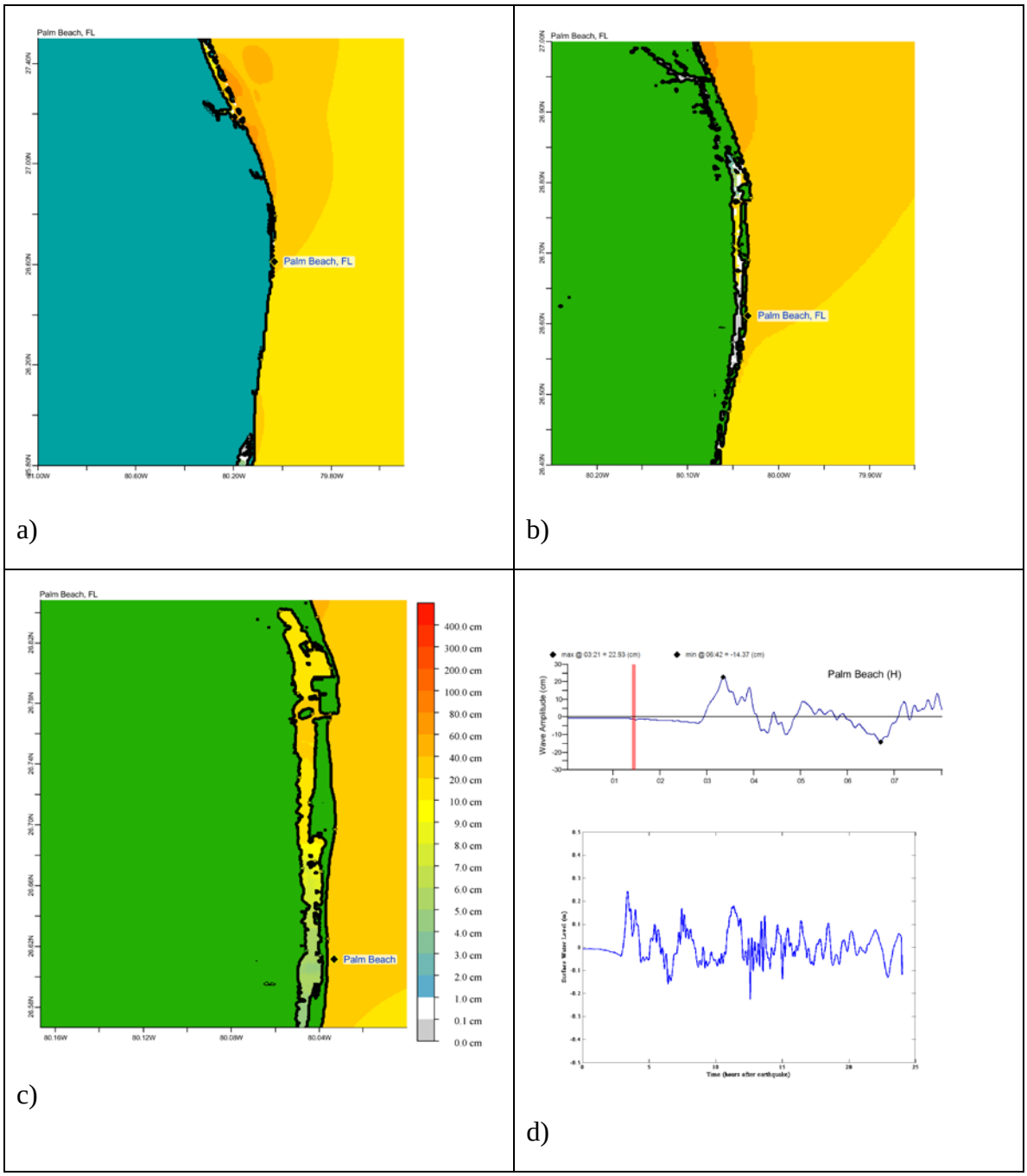

Figure C.1. Response of the Palm Beach forecast model to synthetic scenario ATSZ 38–47 (alpha=30). Maximum sea surface elevation for (a) A grid, (b) B grid, and (c) C grid. Sea surface elevation time series at the C-grid warning point (d). The lower time series plot is the result obtained during model development and is shown for comparison with test results.

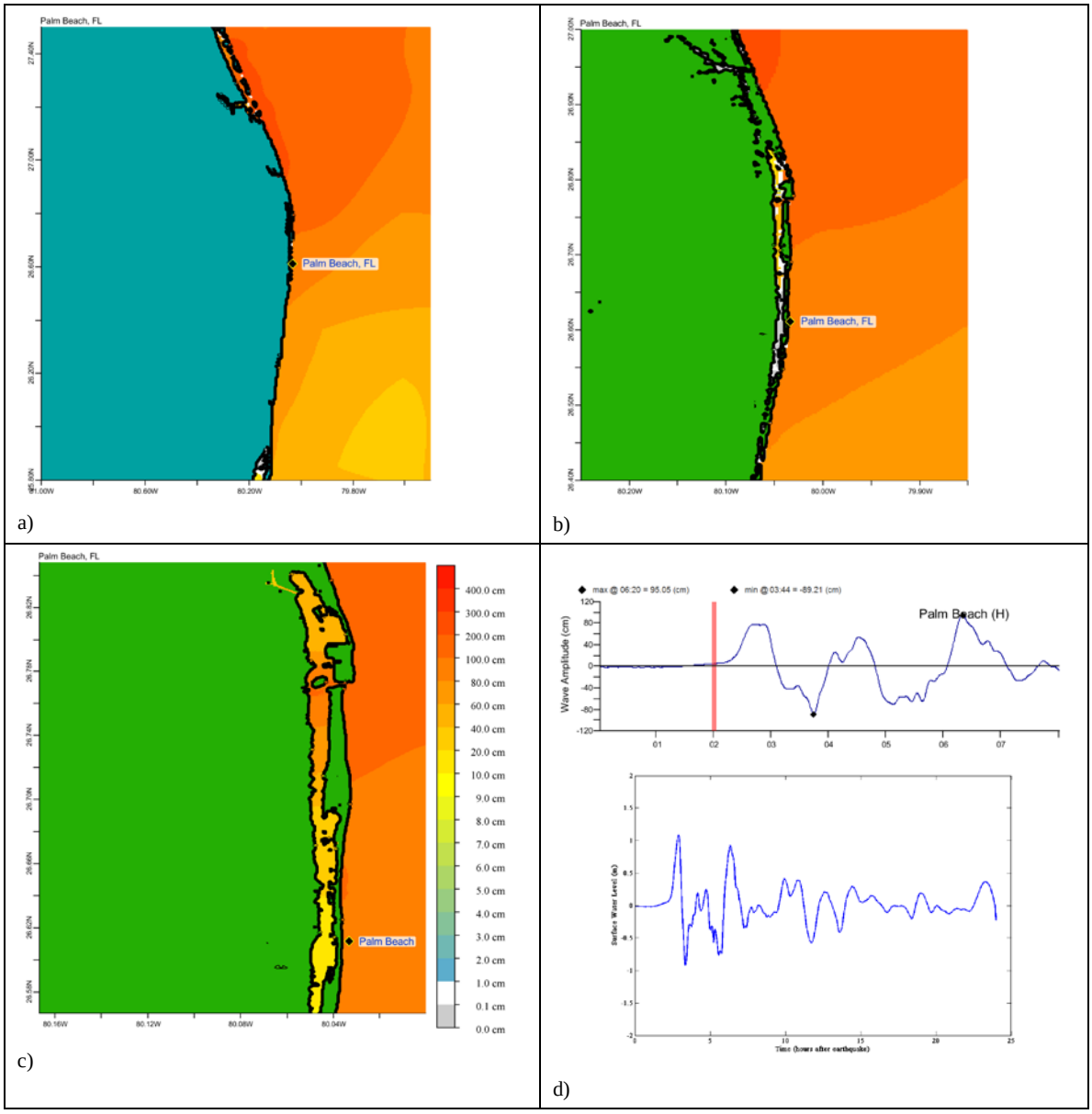

Figure C.2 Response of the Palm Beach forecast model to synthetic scenario ATSZ 48–57 (alpha=30). Maximum sea surface elevation for (a) A grid, (b) B grid, and (c) C grid. Sea surface elevation time series at the C-grid warning point (d). The lower time series plot is the result obtained during model development and is shown for comparison with test results.

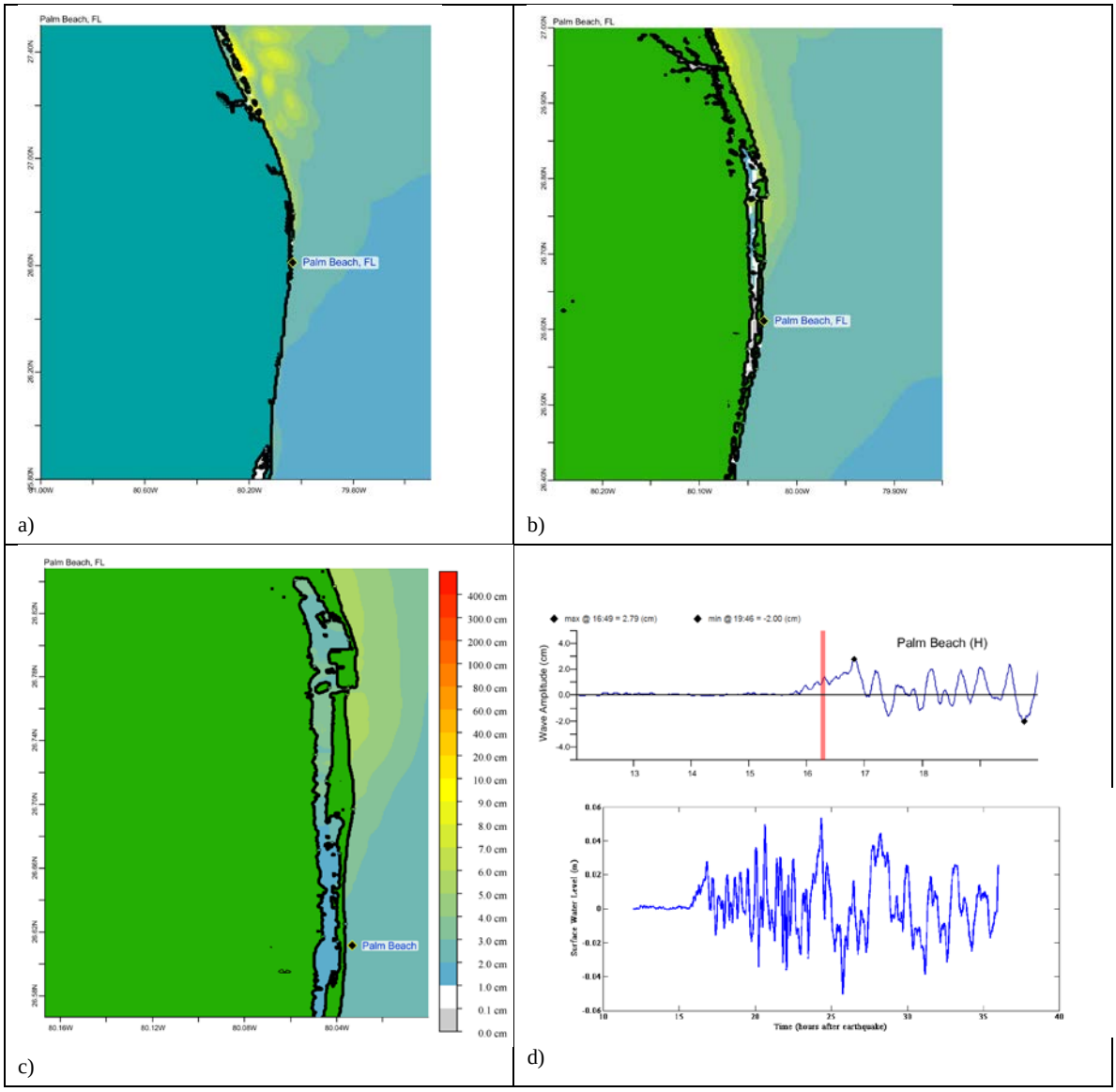

Figure C.3. Response of the Palm Beach forecast model to synthetic scenario SSSZ 1–10 (alpha=30). Maximum sea surface elevation for (a) A grid, (b) B grid, and (c) C grid. Sea surface elevation time series at the C-grid warning point (d). The lower time series plot is the result obtained during model development and is shown for comparison with test results.

Glossary

Arrival time The time when the first tsunami wave is observed at a particular location, typically given in local and/or universal time, but also commonly noted in minutes or hours relative to the time of the earthquake.

Bathymetry The measurement of water depth of an undisturbed body of water.

Cascadia Subduction Zone Fault that extends from Cape Mendocino in Northern California northward to mid-Vancouver Island, Canada. The fault marks the convergence boundary where the Juan de Fuca tectonic plate is being subducted under the margin of the North America plate.

Current speed The scalar rate of water motion measured as distance/time.

Current velocity Movement of water expressed as a vector quantity. Velocity is the distance of movement per time coupled with direction of motion.

Deep-ocean Assessment and Reporting of Tsunamis (DART®) Tsunami detection and transmission system that measures the pressure of an overlying column of water and detects the passage of tsunami.

Digital Elevation Model (DEM) A digital representation of bathymetry or topography based on regional survey data or satellite imagery. Data are arrays of regularly spaced elevations referenced to a map projection of the geographic coordinate system.

Epicenter The point on the surface of the earth that is directly above the focus of an earthquake.

Far-field Region outside of the source of a tsunami where no direct observations of the tsunami-generating event are evident, except for the tsunami waves themselves.

Focus The point beneath the surface of the earth where a rupture or energy release occurs due to a buildup of stress or the movement of earth's tectonic plates relative to one another.

Inundation The horizontal inland extent of land that a tsunami penetrates, generally measured perpendicularly to a shoreline.

Marigram Tide gauge recording of wave level as a function of time at a par ticular location. The instrument used for recording is termed a marigraph.

Method of Splitting Tsunami (MOST) A suite of numerical simulation codes used to provide estimates of the three processes of tsunami evolution: tsunami generation, propagation, and inundation.

Moment magnitude (M_w) The magnitude of an earthquake on a logarithmic scale in terms of the energy released. Moment magnitude is based on the size and characteristics of a fault rupture as determined from long-period seismic waves.

Near–field Region of primary tsunami impact near the source of the tsunami. The near-field is defined as the region where non-tsunami effects of the tsunami-generating event have been observed, such as earth shaking from the earthquake, visible or measured ground deformation, or other direct (non-tsunami) evidences of the source of the tsunami wave.

Propagation database A basin-wide database of pre-computed water elevations and flow velocities at uniformly spaced grid points throughout the world oceans. Values are computed from tsunamis generated by earthquakes with a fault rupture at any one of discrete 100 × 50 km unit sources along worldwide subduction zones.

Runup Vertical difference between the elevation of tsunami inundation and the sea level at the time of a tsunami. Runup is the elevation of the highest point of land inundated by a tsunami as measured relative to a stated datum, such as mean sea level.

Short-term Inundation Forecasting for Tsunamis (SIFT) A tsunami forecast system that integrates tsunami observations in the deep ocean with numerical models to provide an estimate of tsunami wave arrival and amplitude at specific coastal locations while a tsunami propagates across an ocean basin.

Subduction zone A submarine region of the earth's crust at which two or more tectonic plates converge to cause one plate to sink under another, overriding plate. Subduction zones are regions of high seismic activity.

Synthetic event Hypothetical events based on computer simulations or theory of possible or even likely future scenarios.

Tele–tsunami or **distant tsunami** or **far–field tsunami** Most commonly, a tsunami originating from a source greater than 1000 km away from a particular location. In some contexts, a tele-tsunami is one that propagates through deep ocean before reaching a particular location without regard to distance separation.

Tidal wave Term frequently used incorrectly as a synonym for tsunami. A tsunami is unrelated to the predictable periodic rise and fall of sea level due to the gravitational attractions of the moon and sun (see **Tide**, below).

Tide The predictable rise and fall of a body of water (ocean, sea, bay, etc.) due to the gravitational attractions of the moon and sun.

Tide gauge An instrument for measuring the rise and fall of a column of water over time at a particular location.

Travel time The time it takes for a tsunami to travel from the generating source to a particular location.

Tsunameter An oceanographic instrument used to detect and measure tsunamis in the deep ocean. Tsunami measurements are typically transmitted acoustically to a surface buoy that in turn relays them in real time to ground stations via satellite.

Tsunami A Japanese term that literally translates to "harbor wave." Tsunamis are a series of long-period shallow water waves that are generated by the sudden displacement of water due to subsea disturbances such as earthquakes, submarine landslides, or volcanic eruptions. Less commonly, meteoric impact to the ocean or meteorological forcing can generate a tsunami.

Tsunami hazard assessment A systematic investigation of seismically active regions of the world oceans to determine their potential tsunami impact at a particular location. Numerical models are typically used to characterize tsunami generation, propagation, and inundation, and to quantify the risk posed to a particular community from tsunamis generated in each source region investigated.

Tsunami magnitude A number that characterizes the strength of a tsunami based on the tsunami wave amplitudes. Several different tsunami magnitude determination methods have been proposed.

Tsunami propagation The directional movement of a tsunami wave outward from the source of generation. The speed at which a tsunami propagates depends on the depth of the water column in which the wave is traveling. Tsunamis travel at a speed of 700 km/hr (450 mi/hr) over the average depth of 4000 m in the open deep Pacific Ocean.

Tsunami source Location of tsunami origin, most typically an underwater earthquake epicenter. Tsunamis are also generated by submarine landslides, underwater volcanic eruptions, or, less commonly, by meteoric impact of the ocean.

Wall-clock time The time that passes on a common clock or watch between the start and end of a model run, as distinguished from the time needed by a CPU or computer processor to complete the run, typically less than wall-clock time.

Wave amplitude The maximum vertical rise or drop of a column of water as measured from wave crest (peak) or trough to a defined mean water level state.

Wave crest or peak The highest part of a wave or maximum rise above a defined mean water level state, such as mean lower low water.

Wave height The vertical difference between the highest part of a specific wave (crest) and its corresponding lowest point (trough).

Wavelength The horizontal distance between two successive wave crests or troughs.

Wave period The length of time between the passage of two successive wave crests or troughs as measured at a fixed location.

Wave trough The lowest part of a wave or the maximum drop below a defined mean water level state, such as mean lower low water.